

General Optimal Step-size for ADMM-type Algorithms: Domain Parametrization and Optimal Rates

Yifan Ran

Abstract

In this work, we solve a 49-year open problem, the general optimal step-size for ADMM-type algorithms. For a convex program: $\min. f(\mathbf{x}) + g(\mathbf{z})$, s.t. $\mathcal{A}\mathbf{x} - \mathcal{B}\mathbf{z} = \mathbf{c}$, given an arbitrary fixed-point initialization ζ^0 , an optimal step-size choice is given by a root of the following polynomial:

$$\rho^4 \|\mathcal{A}\mathbf{x}^*\|^2 - \rho^3 \langle \mathcal{A}\mathbf{x}^*, \zeta^0 \rangle + \rho \langle \lambda^*, \zeta^0 \rangle - \|\lambda^*\|^2 = 0,$$

with $\rho \neq 0$ a domain step-size, which relates to the classical positive one via $\gamma = \rho^2$. We denote by \cdot^* the optimal solution, by λ the Lagrange multiplier associated with the equality constraint (dual variable).

The above polynomial always admits a closed-form solution. The optimality is in the sense that a worst-case fixed-point convergence rate is minimized, which is a balance of the normalized primal and dual iterates convergence speed (reciprocally related). In cases where either the primal or dual solution is trivial (a zero vector), improvement can be made by accelerating the non-trivial sequence only.

For practical use, adaptively replace the above optimal solutions with the current iterates, which are known at every iteration. Numerically, it exhibits almost identical performance as the theoretical one (after a few iterations), similar to the underlying best fixed step-size (found by exhaustive grid search).

Keywords: Proximal operator, Duality, Fixed-point theory, Bounded linear operators, Range and domain parametrizations, Primal-dual solution angle, Initialization angle, Firm non-expansiveness, Alternating direction method of multipliers (ADMM).

Mathematics Subject Classification (2020) 90C25, 90C06, 65K05, 65F22

1 Introduction

An ongoing trend referred to as ‘Big Data’ is drawing an increasing amount of attention from both industry and academia. How to efficiently handle the explosion of data is of central importance. In the review paper by Stephen Boyd et al. [1], the Alternating Direction Method of Multipliers (ADMM) is recommended: ‘*It is well suited to distributed convex optimization, and in particular to large-scale problems arising in statistics, machine learning, and related areas.*’ The ADMM algorithm was introduced by Glowinski and Marrocco [2]

The author is with the department of Electrical and Electronics Engineering, Imperial College London, UK (e-mail: y.ran18@imperial.ac.uk).

in 1975, and Gabay and Mercier [3] in 1976, with roots in the 1950s. The algorithm was studied throughout the 1980s, and by the mid-1990s, most of the theoretical results were established [1].

One theoretical consequence is that ADMM will converge with arbitrary positive step-size choices. Interestingly, all these choices, along with their corresponding iteration number complexity, seem to roughly form a convex graph, implying the feasibility of determining the best choice by convex optimization techniques [4, 5]. However, how to formulate the general convex program and then solve for its optimal solution has been a mystery. Challengingly, numerical experiments show that the underlying best fixed step-size can take any positive values, from extremely small to arbitrarily large, related to problem structures and data sizes. Particularly, the best choice does not generally translate to alternative formulations or data sets. It is hard to see any pattern and hence difficult to guess a good choice. Meanwhile, a good step-size can largely improve the algorithm’s efficiency. It is therefore of both theoretical and practical interest to determine the optimal step-size choice.

Unfortunately, the ADMM optimal step-size is one of the very few issues that have not been addressed in the last 49 years. As pointed out in a recent paper by Bartolomeo Stellato and Stephen Boyd et al. [6, sec. 1.2, First-order methods] ‘*Despite some recent theoretical results [7, 8], it remains unclear how to select those parameters to optimize the algorithm convergence rate*’. The same open problem is also mentioned by Ernest K. Ryu and Wotao Yin in [9, Sec. 8, Parameter selection].

In this work, we provide a general, worst-case optimal choice, without the need for any tailored structure information. It is simple, universally applicable, highly efficient, and practically useful. The key is to introduce the *domain parametrization*, i.e., associating the step-size parameter to the domain of a function. This is in contrast to the current literature where one assigns the parameter to the range, i.e., the left-hand side. We argue that the classical range association is not mathematically natural, in the sense that an extra, implicit, step-size-related scaling arises, which shifts the algorithm sequence to a parallel variant. Such parallelism does not affect any practical uses, since all convergence properties (such as rates, step-size choices) will be the same. However, it would cause a strong barrier to finding the general theoretical optimal step-size. While this issue is not obvious, there does exist a hint from the well-known Moreau identity — its original symmetry is lost after the classical parametrization. Such extra scaling/shifting will be naturally avoided by the *domain parametrization*. In fact, there are more benefits to our new parametrization. We will present some new, simple, highly unified analyses for the ADMM-type algorithms, and draw several useful conclusions.

After finding the optimal step-size, we can invoke it to obtain some optimal convergence rates, which reveal that (i) under zero initialization, the ADMM efficiency is intrinsically characterized by the angle between the primal and dual solutions; (ii) if either the primal or dual solution is trivial (a zero vector), then under zero initialization, the non-trivial iterate convergence speed is independent of the step-size choice; (iii) meanwhile, in the same partly-trivial setting, if instead employ an arbitrary non-zero initialization. Then, invoke a corresponding optimal step-size, we show that the non-trivial iterate convergence rate will be improved by a factor of $\sin^2 \omega \in [0, 1]$, where ω is the angle between the initialization and the non-trivial solution. Particularly, when $\omega = 0$ or $\omega = \pi$, we obtain $\sin^2 \omega = 0$, and the algorithm converges instantly, implying the initialization is optimal. This last case

also implies that only the initial angle matters, due to the distance will be automatically adjusted by a closed-form optimal step-size.

Our optimal step-size changes with different initializations, and a good initialization choice can be shown to improve the algorithm efficiency. In the literature, how to estimate a good initialization has been intensively studied, referred to as the ‘warm start’. Typical success is regarding the type of problems that sequentially apply ADMM. The reason for the repeat application of ADMM can be due to decisions need updating as the scenario changes dynamically. In this case, one can directly adopt the solution from the previous ADMM as an initialization for the next one, see e.g. [10]. Another class of problems is clustering and dictionary learning. Typically, there is an outer and an inner loop. One can directly use the output of each inner loop as a warm start for the next one, see e.g. [11]. At last, one can apply machine learning to find a near-optimal initialization in a general sense, typical work can be found by Bartolomeo Stellato et. al. [12, 13], see also [14] on a power flow problem.

At last, our results are transferable owing to the equivalence of ADMM and many other algorithms. The most well-known equivalence is perhaps with the Douglas-Rachford splitting (DRS) [15] from numerical analysis. It is widely recognized that ADMM iterates are equivalent to applying DRS to its dual problem, see e.g. [16, 17]. Recently, Daniel O’Connor and Lieven Vandenbergh [18] show that the Primal-Dual Hybrid Gradient (PDHG) method [19, 20, 21] is also equivalent to ADMM. Apart from being equivalent, there are many closely related algorithms such as Spingarn’s method of partial inverses, Dykstra’s alternating projections method, and Bregman iterative algorithms for l_1 problems in signal processing, see more details from the review paper [1].

1.1 Notations

We use blackboard bold letters such as \mathbb{H} to denote a real Hilbert space with inner product $\langle \cdot, \cdot \rangle$ and norm $\|\cdot\|$ equipped. The uppercase calligraphic letters are used to denote bounded linear operators. Particularly, \mathcal{I} always denotes the identity operator. An operator \mathcal{A} on a Hilbert space is a point-to-set mapping $\mathcal{A} : \mathbb{H} \rightarrow 2^{\mathbb{H}}$. We denote by $\Gamma_0(\mathbb{H})$ the space of convex, closed and proper (CCP) functions from \mathbb{H} to the extended real line $(-\infty, +\infty]$, by $\mathfrak{B}(\mathbb{H}, \mathbb{K})$ the space of bounded linear operators from domain \mathbb{H} to range \mathbb{K} , by \circ the operator or function composition, by $\text{dom}(\cdot)$ the domain, by $\text{ran}(\cdot)$ the range, by \emptyset the empty set. The adjoint of an operator $\mathcal{A} \in \mathfrak{B}(\mathbb{H}, \mathbb{K})$ is the unique operator $\mathcal{A}^* \in \mathfrak{B}(\mathbb{K}, \mathbb{H})$ satisfying $\langle \mathcal{A}\mathbf{x}, \mathbf{y} \rangle = \langle \mathbf{x}, \mathcal{A}^*\mathbf{y} \rangle$, $\forall \mathbf{x} \in \mathbb{H}, \forall \mathbf{y} \in \mathbb{K}$. The Fenchel conjugate function is defined as $f^*(\cdot) = \sup \langle \mathbf{z}, \cdot \rangle - f(\mathbf{z})$. The uppercase bold, lowercase bold, and not bold letters are used for matrices, vectors, and scalars, respectively.

1.2 ADMM algorithm

ADMM solves the following general convex problem:

$$\begin{aligned} & \underset{\mathbf{x}, \mathbf{z}}{\text{minimize}} && f(\mathbf{x}) + g(\mathbf{z}), \\ & \text{subject to} && \mathcal{A}\mathbf{x} - \mathcal{B}\mathbf{z} = \mathbf{c}, \end{aligned} \tag{1.1}$$

with variables $\mathbf{x} \in \mathbb{H}$, $\mathbf{z} \in \mathbb{P}$, $\mathbf{c} \in \mathbb{K}$ and functions $f \in \Gamma_0(\mathbb{H})$, $g \in \Gamma_0(\mathbb{P})$, where $\mathcal{A} \in \mathfrak{B}(\mathbb{H}, \mathbb{K})$ and $\mathcal{B} \in \mathfrak{B}(\mathbb{P}, \mathbb{K})$ are injective. A solution is assumed exists.

The augmented Lagrangian is

$$\mathcal{L}_\gamma(\mathbf{x}, \mathbf{z}, \boldsymbol{\lambda}) = f(\mathbf{x}) + g(\mathbf{z}) + \frac{\gamma}{2} \|\mathcal{A}\mathbf{x} - \mathcal{B}\mathbf{z} - \mathbf{c} + \boldsymbol{\lambda}/\gamma\|^2, \quad (1.2)$$

with $\gamma > 0$ being a positive step-size. The classical ADMM iterates are

$$\mathbf{x}^{k+1} = \underset{\mathbf{x}}{\operatorname{argmin}} \mathcal{L}_\gamma(\mathbf{x}, \mathbf{z}^k, \boldsymbol{\lambda}^k), \quad (\text{primal})$$

$$\mathbf{z}^{k+1} = \underset{\mathbf{z}}{\operatorname{argmin}} \mathcal{L}_\gamma(\mathbf{x}^{k+1}, \mathbf{z}, \boldsymbol{\lambda}^k), \quad (\text{auxiliary})$$

$$\boldsymbol{\lambda}^{k+1} = \boldsymbol{\lambda}^k + \gamma(\mathcal{A}\mathbf{x}^{k+1} - \mathcal{B}\mathbf{z}^{k+1} - \mathbf{c}), \quad (\text{dual})$$

where $k = 0, 1, \dots$ denotes the iteration number counter.

Additionally, the above 3-steps algorithm can be rewritten into a 1-step fixed-point characterization:

$$\boldsymbol{\zeta}_1^{k+1} = \mathcal{F}_\gamma \boldsymbol{\zeta}_1^k, \quad (1.3)$$

where \mathcal{F}_γ is a certain γ -related operator detailed later, and where $\boldsymbol{\zeta}_1$ denotes a fixed-point variable, with a classical expression associated with (1.1) being

$$\boldsymbol{\zeta}_1^{k+1} = \mathcal{A}\mathbf{x}^{k+1} + \boldsymbol{\lambda}^k/\gamma. \quad (\text{classical fixed-point})$$

Moreover, the above \mathcal{F}_γ is well-known to be firmly non-expansive (defined below), see e.g. [9, 22].

Definition 1.1. *Let $\mathcal{F} : \mathbb{H} \rightarrow \mathbb{H}$. Then, \mathcal{F} is firmly non-expansive if*

$$\|\mathcal{F}\mathbf{x} - \mathcal{F}\mathbf{y}\|^2 \leq \langle \mathcal{F}\mathbf{x} - \mathcal{F}\mathbf{y}, \mathbf{x} - \mathbf{y} \rangle, \quad \forall \mathbf{x}, \mathbf{y} \in \mathbb{H}. \quad (1.4)$$

1.3 Key results

1.3.1 open problem (theoretical)

The general optimal step-size remains open in the last 49 years for ADMM (and 68 years for DRS), see [6, Sec. 1.2, First-order methods], [9, Sec. 8, Parameter selection]. In this work, we provide a universally applicable optimal choice as a closed-form root of the following polynomial:

$$\rho^4 \|\mathcal{A}\mathbf{x}^\star\|^2 - \rho^3 \langle \mathcal{A}\mathbf{x}^\star, \boldsymbol{\zeta}^0 \rangle + \rho \langle \boldsymbol{\lambda}^\star, \boldsymbol{\zeta}^0 \rangle - \|\boldsymbol{\lambda}^\star\|^2 = 0, \quad (1.5)$$

with $\rho \neq 0$ denotes a domain step-size, which relates to the classical one as in (1.2) via $\gamma = \rho^2$, where $\boldsymbol{\zeta}^0 = \rho_0 \mathcal{A}\mathbf{x}^0 + \boldsymbol{\lambda}^0/\rho_0$ is an arbitrarily fixed-point initialization, and where \mathbf{x}^0 , $\boldsymbol{\lambda}^0$, and ρ_0 denote the primal iterate, dual iterate, and the step-size initial choice, respectively.

The above step-size selection does not incorporate any tailored structure information, and is therefore only optimal in a worst-case sense. Nevertheless, numerically, we observe that it is already close to the underlying best fixed choice in all our experiments (found by exhaustive grid search), seemingly sufficient for basic practical usages.

1.3.2 practical use

For practical use, solve the following polynomial at every $(k + 1)$ -th iteration:

$$\rho^4 \|\mathcal{A}\mathbf{x}^{k+1}\|^2 - \rho^3 \langle \mathcal{A}\mathbf{x}^{k+1}, \zeta^0 \rangle + \rho \langle \boldsymbol{\lambda}^{k+1}, \zeta^0 \rangle - \|\boldsymbol{\lambda}^{k+1}\|^2 = 0, \quad (1.6)$$

see more details from Sec. 4.5. Numerically, it exhibits highly similar performance as the above theoretical one (almost identical after a few iterations, typically $k = 10$).

For ease of use, below we present the simplest version, expressed in terms of the classical step-size $\gamma > 0$.

Algorithm 1 ADMM with adaptive step-sizes (Simplified version)

Input: Set $\mathbf{z}^0 = \mathbf{0}$, $\boldsymbol{\lambda}^0 = \mathbf{0}$, $\gamma_0 = 1$.

1: **while** iteration $k = 0, 1, 2, \dots$ **do**

2:

$$\mathbf{x}^{k+1} = \underset{\mathbf{x}}{\operatorname{argmin}} f(\mathbf{x}) + \frac{\gamma_k}{2} \|\mathcal{A}\mathbf{x} - \mathcal{B}\mathbf{z}^k - \mathbf{c} + \boldsymbol{\lambda}^k / \gamma_k\|^2, \quad (1.7)$$

$$\mathbf{z}^{k+1} = \underset{\mathbf{z}}{\operatorname{argmin}} g(\mathbf{z}) + \frac{\gamma_k}{2} \|\mathcal{A}\mathbf{x}^{k+1} - \mathcal{B}\mathbf{z} - \mathbf{c} + \boldsymbol{\lambda}^k / \gamma_k\|^2, \quad (1.8)$$

$$\boldsymbol{\lambda}^{k+1} = \boldsymbol{\lambda}^k + \gamma_k (\mathcal{A}\mathbf{x}^{k+1} - \mathcal{B}\mathbf{z}^{k+1} - \mathbf{c}), \quad (1.9)$$

$$\gamma_{k+1} = \|\boldsymbol{\lambda}^{k+1}\| / \|\mathcal{A}\mathbf{x}^{k+1}\|. \quad (1.10)$$

3: **end while**

Output: primal and dual solutions \mathbf{x}^* and $\boldsymbol{\lambda}^*$, respectively.

1.3.3 unscaled fixed-point

In the iterate, there exist two fixed-point expressions for ADMM-type algorithms:

$$\underbrace{\zeta_1^* = \mathcal{A}\mathbf{x}^* + \boldsymbol{\lambda}^* / \gamma}_{\text{for primal problem}}, \quad \underbrace{\zeta_2^* = \gamma \mathcal{A}\mathbf{x}^* + \boldsymbol{\lambda}^*}_{\text{for dual problem}}. \quad (1.11)$$

see ζ_1^* from e.g. [9, sec. 3.1], corresponding to the primal problem, and ζ_2^* from e.g. [9, sec. 3.2], [22], corresponding to the Fenchel dual problem.

In this work, we show that the above expressions lead to self-contradicted step-size choices, see Sec. 4.1.1. This is due to that they are both implicitly scaled/shifted, and the unscaled version is

$$\zeta^* = \rho \mathcal{A}\mathbf{x}^* + \boldsymbol{\lambda}^* / \rho, \quad (\text{unscaled})$$

where $\rho = \pm\sqrt{\gamma}$ is our domain step-size, see derivation from Proposition 2.5, and proof of being unscaled in Sec. 2.8.2 via self-duality.

1.3.4 Some optimal rates

Below, we present some convergence rates, induced by certain optimal step-sizes.

- First, a general case with zero initialization, see theoretical details from Sec. 4.3.1 and numerical verifications through Lasso in Sec. 5.1:

(i) (Balanced rates.) Suppose $\mathbf{x}^* \neq \mathbf{0}$, $\boldsymbol{\lambda}^* \neq \mathbf{0}$, i.e., $\|\mathcal{A}\mathbf{x}^*\| \neq 0$, $\|\boldsymbol{\lambda}^*\| \neq 0$ (\mathcal{A} assumed injective). Set initialization $\boldsymbol{\zeta}^0 = \mathbf{0}$. Let

$$\theta = \arccos \frac{\langle \mathcal{A}\mathbf{x}^*, \boldsymbol{\lambda}^* \rangle}{\|\mathcal{A}\mathbf{x}^*\| \|\boldsymbol{\lambda}^*\|}. \quad (\text{intrinsic angle})$$

Choose domain step-size to be $\rho^* = \pm \sqrt{\|\boldsymbol{\lambda}^*\| / \|\mathcal{A}\mathbf{x}^*\|}$. Then,

$$\frac{\|\mathcal{A}\mathbf{x}^{k+2} - \mathcal{A}\mathbf{x}^{k+1}\|^2}{\|\mathcal{A}\mathbf{x}^*\|^2} \leq \frac{2}{k+1} (1 + \cos \theta), \quad (\text{primal})$$

$$\frac{\|\boldsymbol{\lambda}^{k+1} - \boldsymbol{\lambda}^k\|^2}{\|\boldsymbol{\lambda}^*\|^2} \leq \frac{2}{k+1} (1 + \cos \theta), \quad (\text{dual})$$

$$\frac{\|\boldsymbol{\zeta}^{k+1} - \boldsymbol{\zeta}^k\|^2}{\|\mathcal{A}\mathbf{x}^*\| \|\boldsymbol{\lambda}^*\|} \leq \frac{2}{k+1} (1 + \cos \theta). \quad (\text{fixed-point})$$

• Next, a special case where the dual solution is a zero vector, see theoretical details from Sec. 4.3.2 and numerical verifications through a feasibility problem in Sec. 5.2:

(ii) (Fixed non-trivial rate.) Suppose $\|\mathcal{A}\mathbf{x}^*\| \neq 0$, $\|\boldsymbol{\lambda}^*\| = 0$. Set initialization $\boldsymbol{\zeta}^0 = \mathbf{0}$. Then,

$$\|\mathcal{A}\mathbf{x}^{k+2} - \mathcal{A}\mathbf{x}^{k+1}\|^2 \leq \frac{1}{k+1} \cdot \|\mathcal{A}\mathbf{x}^*\|^2, \quad (\text{non-trivial primal})$$

$$\|\boldsymbol{\lambda}^{k+1} - \boldsymbol{\lambda}^k\|^2 \leq \frac{1}{k+1} \cdot \|\mathcal{A}\mathbf{x}^*\|^2 \cdot \rho^4, \quad (\text{trivial dual})$$

$$\|\boldsymbol{\zeta}^{k+1} - \boldsymbol{\zeta}^k\|^2 \leq \frac{1}{k+1} \cdot \|\mathcal{A}\mathbf{x}^*\|^2 \cdot \rho^2, \quad (\text{fixed-point})$$

where the optimal step-size is $\rho^* \rightarrow 0$, which only affect the dual and fixed-point sequences.

(iii) (Guaranteed non-trivial improvement.) Suppose $\|\mathcal{A}\mathbf{x}^*\| \neq 0$, $\|\boldsymbol{\lambda}^*\| = 0$. Set any initialization $\boldsymbol{\zeta}^0 \neq \mathbf{0}$. Let

$$\omega_1 = \arccos \frac{\langle \mathcal{A}\mathbf{x}^*, \boldsymbol{\zeta}^0 \rangle}{\|\mathcal{A}\mathbf{x}^*\| \|\boldsymbol{\zeta}^0\|}. \quad (\text{initial angle})$$

Choose domain step-size to be $\rho_{\text{pri}}^* = \|\boldsymbol{\zeta}^0\| / (\|\mathcal{A}\mathbf{x}^*\| \cos \omega_1)$. Then,

$$\|\mathcal{A}\mathbf{x}^{k+2} - \mathcal{A}\mathbf{x}^{k+1}\|^2 \leq \frac{1}{k+1} \cdot \|\mathcal{A}\mathbf{x}^*\|^2 \cdot \sin^2 \omega_1, \quad (\text{non-trivial primal})$$

$$\|\boldsymbol{\lambda}^{k+1} - \boldsymbol{\lambda}^k\|^2 \leq \frac{1}{k+1} \cdot \frac{\|\boldsymbol{\zeta}^0\|^4}{\|\mathcal{A}\mathbf{x}^*\|^2} \cdot \frac{\tan^2 \omega_1}{\cos^2 \omega_1}, \quad (\text{trivial dual})$$

$$\|\boldsymbol{\zeta}^{k+1} - \boldsymbol{\zeta}^k\|^2 \leq \frac{1}{k+1} \cdot \|\boldsymbol{\zeta}^0\|^2 \cdot \tan^2 \omega_1. \quad (\text{fixed-point})$$

Similar results hold for a symmetric situation where $\|\mathcal{A}\mathbf{x}^*\| = 0$, $\|\boldsymbol{\lambda}^*\| \neq 0$.

1.4 Organization

In Sec. 2, we introduce a new domain-type parametrization and several useful consequences on the proximal operator and the ADMM algorithm. Sec. 3 establishes some convergence rates. Sec. 4 presents the optimal step-sizes by minimizing worst-case convergence rates. Sec. 5 conducts two numerical experiments to verify our results.

2 Two parametrizations: range and domain types

In this section, we introduce a new domain-type parametrization, parallel to the classical range-type parametrization. We show that the classical way introduces an implicit, extra, and step-size-related scaling, causing the 49-year optimal step-size open problem. This issue will be naturally avoided by our new parametrization.

2.1 Fundamental ground

Throughout the paper, we will repeatedly use a standard tool, the proximal operator, which is widely used across fields, see a survey paper [23]. It is developed as a generalization of the projector (onto convex sets) by Moreau [24], defined as (without parametrization):

Definition 2.1. *Given $f \in \Gamma_0(\mathbb{H})$, $\text{dom}(f) \neq \emptyset$, the proximal operator is defined as*

$$\mathbf{Prox}_f(\mathbf{v}) = \underset{\mathbf{z}}{\operatorname{argmin}} f(\mathbf{z}) + \frac{1}{2}\|\mathbf{z} - \mathbf{v}\|^2, \quad (2.1)$$

where $\|\cdot\|$ denotes the Euclidean norm, and where $\text{dom}(\cdot)$ denotes the domain.

An important relation is the following Moreau identity:

$$\mathbf{v} = \mathbf{Prox}_f(\mathbf{v}) + \mathbf{Prox}_{f^*}(\mathbf{v}), \quad (2.2)$$

where $f^*(\cdot) \stackrel{\text{def}}{=} \sup \langle \mathbf{z}, \cdot \rangle - f(\mathbf{z})$ is the Fenchel conjugate function. The above is an important link for primal and dual problems.

2.2 Classical range parametrization

It is standard to consider a parametrized version of the proximal operator.

Definition 2.2. *Given $f \in \Gamma_0(\mathbb{H})$, $\text{dom}(f) \neq \emptyset$. Let $\gamma > 0$ denote a positive step-size. Then, the γ -parametrized proximal operator is*

$$\mathbf{Prox}_{\gamma f}(\mathbf{v}) = \underset{\mathbf{z}}{\operatorname{argmin}} \gamma f(\mathbf{z}) + \frac{1}{2}\|\mathbf{z} - \mathbf{v}\|^2 = \underset{\mathbf{z}}{\operatorname{argmin}} f(\mathbf{z}) + \frac{1}{2\gamma}\|\mathbf{z} - \mathbf{v}\|^2. \quad (2.3)$$

The Moreau identity becomes

$$\mathbf{v} = \mathbf{Prox}_{\gamma f}(\mathbf{v}) + \left(\gamma \mathcal{I} \right) \circ \mathbf{Prox}_{\frac{1}{\gamma} f^*} \circ \left(\frac{1}{\gamma} \mathcal{I} \right) (\mathbf{v}), \quad (2.4)$$

where $\mathcal{I} : \mathbb{H} \rightarrow \mathbb{H}$ denotes the identity operator.

Remarks 2.1 (hint: extra scaling). Compare (2.4) and (2.2), we see that — after parametrization, the Moreau identity components are no longer symmetric, with an extra $\gamma(\cdot)^{\frac{1}{\gamma}}$ type structure. This seemingly inconsequential phenomenon contains an important hint on the step-size open problem — an extra scaling.

2.3 Domain parametrization

We note that conventionally one always assigns the step-size to the range of a function. Here, we introduce a symmetric domain-type parametrization.

Proposition 2.1. *Given $f \in \Gamma_0(\mathbb{H})$, $\text{dom}(f) \neq \emptyset$ and scalar $\rho \neq 0$, the domain-parametrized proximal operator is*

$$\begin{aligned} \mathbf{Prox}_{f\rho}(\mathbf{v}) &= \underset{\mathbf{z}_1 \in \mathbb{H}}{\operatorname{argmin}} f(\rho \mathbf{z}_1) + \frac{1}{2} \|\mathbf{z}_1 - \mathbf{v}\|^2, \\ &= \frac{1}{\rho} \underset{\mathbf{z}_2 \in \mathbb{H}}{\operatorname{argmin}} f(\mathbf{z}_2) + \frac{1}{2} \left\| \frac{\mathbf{z}_2}{\rho} - \mathbf{v} \right\|^2. \end{aligned} \quad (2.5)$$

Proof. The second equality is obtained via a variable substitution $\mathbf{z}_2 = \rho \mathbf{z}_1$. \square

Lemma 2.1 (translation rule). *The classical proximal operator as in (2.3) and our domain-parametrized version (2.5) are related via*

$$\mathbf{Prox}_{f\rho}(\mathbf{v}) = \left(\frac{1}{\rho} \mathcal{I} \right) \circ \mathbf{Prox}_{\rho^2 f} \circ \left(\rho \mathcal{I} \right) (\mathbf{v}), \quad \rho \neq 0 \quad (2.6)$$

$$\mathbf{Prox}_{\gamma f}(\mathbf{v}) = \left(\pm \sqrt{\gamma} \mathcal{I} \right) \circ \mathbf{Prox}_{f(\pm \sqrt{\gamma})} \circ \left(\pm \frac{1}{\sqrt{\gamma}} \mathcal{I} \right) (\mathbf{v}), \quad \gamma > 0. \quad (2.7)$$

Proof. For the first relation (2.6). From the right-hand side, we obtain

$$\begin{aligned} \left(\frac{1}{\rho} \mathcal{I} \right) \circ \mathbf{Prox}_{\rho^2 f} \circ \left(\rho \mathcal{I} \right) \mathbf{v} &= \frac{1}{\rho} \underset{\mathbf{z}}{\operatorname{argmin}} f(\mathbf{z}) + \frac{1}{2\rho^2} \|\mathbf{z} - \rho \mathbf{v}\|^2, \\ &= \frac{1}{\rho} \underset{\mathbf{z}}{\operatorname{argmin}} f(\mathbf{z}) + \frac{1}{2} \left\| \frac{\mathbf{z}}{\rho} - \mathbf{v} \right\|^2, \end{aligned} \quad (2.8)$$

which coincides with definition (2.5).

For the second relation (2.7), consider the positive sign case. From the right-hand side, we obtain

$$\begin{aligned} \left(\sqrt{\gamma} \mathcal{I} \right) \circ \mathbf{Prox}_{f\sqrt{\gamma}} \circ \left(\frac{1}{\sqrt{\gamma}} \mathcal{I} \right) \mathbf{v} &= \frac{\sqrt{\gamma}}{\sqrt{\gamma}} \underset{\mathbf{z}_2}{\operatorname{argmin}} f(\mathbf{z}_2) + \frac{1}{2} \left\| \frac{\mathbf{z}_2}{\sqrt{\gamma}} - \frac{\mathbf{v}}{\sqrt{\gamma}} \right\|^2, \\ &= \underset{\mathbf{z}_2}{\operatorname{argmin}} f(\mathbf{z}_2) + \frac{1}{2\gamma} \|\mathbf{z}_2 - \mathbf{v}\|^2, \end{aligned} \quad (2.9)$$

which coincides with definition (2.3). For the negative sign, similarly,

$$\begin{aligned} \left(-\sqrt{\gamma} \mathcal{I} \right) \circ \mathbf{Prox}_{f(-\sqrt{\gamma})} \circ \left(\frac{1}{-\sqrt{\gamma}} \mathcal{I} \right) \mathbf{v} \\ = \frac{-\sqrt{\gamma}}{-\sqrt{\gamma}} \underset{\mathbf{z}_2}{\operatorname{argmin}} f(\mathbf{z}_2) + \frac{1}{2} \left\| \frac{\mathbf{z}_2}{-\sqrt{\gamma}} - \frac{\mathbf{v}}{-\sqrt{\gamma}} \right\|^2 = \underset{\mathbf{z}_2}{\operatorname{argmin}} f(\mathbf{z}_2) + \frac{1}{2\gamma} \|\mathbf{z}_2 - \mathbf{v}\|^2, \end{aligned} \quad (2.10)$$

which is the same as definition (2.3). The proof is now concluded. \square

Remarks 2.2 (step-size relation). In view of the above lemma, clearly our domain step-size relates to the classical range step-size via

$$\gamma = \rho^2. \quad (2.11)$$

2.4 Extra scaling

By now, we repeatedly observe $\rho\mathcal{I} \circ (\cdot) \circ \frac{1}{\rho}\mathcal{I}$ type of operations, recall Lemma 2.1 and Moreau identity (2.4). Here, we show that this operation implies shifting. How to remove it is key to our technique.

2.4.1 parallelism

To start, we specify what we mean by ‘extra scaling’.

Let process $\zeta^{k+1} = \mathcal{F}\zeta^k$ generate a sequence $\{\zeta^k\}$, with $k = 0, 1, \dots$ denotes the iteration number counter. Then, given any $\rho \neq 0$, we have

$$\begin{aligned} \zeta^{k+1} = \mathcal{F}\zeta^k, & \iff \zeta^{k+1} = \frac{1}{\rho}\mathcal{I} \circ \left(\rho\mathcal{I} \circ \mathcal{F} \circ \frac{1}{\rho}\mathcal{I} \right) \circ \rho\mathcal{I} (\zeta^k), \\ & \iff (\rho\zeta^{k+1}) = \left(\rho\mathcal{I} \circ \mathcal{F} \circ \frac{1}{\rho}\mathcal{I} \right) (\rho\zeta^k). \end{aligned} \quad (2.12)$$

Lemma 2.2. *Let $\mathcal{F} : \mathbb{H} \rightarrow \mathbb{H}$ be firmly non-expansive. Then, the composited mapping $\rho\mathcal{I} \circ \mathcal{F} \circ \frac{1}{\rho}\mathcal{I}$ with any $\rho \neq 0$ is also firmly nonexpansive.*

Proof. Recall the definition of firm non-expansiveness, restated here as

Definition 2.3. *Let $\mathcal{F} : \mathbb{H} \rightarrow \mathbb{H}$. Then, \mathcal{F} is firmly non-expansive if*

$$\|\mathcal{F}\mathbf{x} - \mathcal{F}\mathbf{y}\|^2 \leq \langle \mathcal{F}\mathbf{x} - \mathcal{F}\mathbf{y}, \mathbf{x} - \mathbf{y} \rangle, \quad \forall \mathbf{x}, \mathbf{y} \in \mathbb{H}. \quad (2.13)$$

It follows that, $\forall \zeta, \mathbf{y} \in \mathbb{H}$, the following holds:

$$\begin{aligned} \|\mathcal{F}\zeta - \mathcal{F}\mathbf{y}\|^2 & \leq \langle \mathcal{F}\zeta - \mathcal{F}\mathbf{y}, \zeta - \mathbf{y} \rangle, \\ \iff \rho^2 \|\mathcal{F}\zeta - \mathcal{F}\mathbf{y}\|^2 & \leq \rho^2 \langle \mathcal{F}\zeta - \mathcal{F}\mathbf{y}, \zeta - \mathbf{y} \rangle, \quad \rho \neq 0, \\ \iff \|\tilde{\mathcal{F}}\tilde{\zeta} - \tilde{\mathcal{F}}\tilde{\mathbf{y}}\|^2 & \leq \langle \tilde{\mathcal{F}}\tilde{\zeta} - \tilde{\mathcal{F}}\tilde{\mathbf{y}}, \tilde{\zeta} - \tilde{\mathbf{y}} \rangle, \end{aligned} \quad (2.14)$$

with substitutions:

$$\tilde{\zeta} = \rho\zeta, \quad \tilde{\mathbf{y}} = \rho\mathbf{y}, \quad \tilde{\mathcal{F}} = \rho\mathcal{I} \circ \mathcal{F} \circ \frac{1}{\rho}\mathcal{I}. \quad (2.15)$$

The proof is now concluded. \square

Lemma 2.3 (ρ -distanced parallel sequences). *Let process $\zeta^{k+1} = \mathcal{F}\zeta^k$ generate a sequence $\{\zeta^k\}$, with iteration number counter $k = 0, 1, 2, \dots$.*

Then, there exist the following ρ -distanced parallel variants:

$$\{\mathbf{y}^k \mid \mathbf{y}^k = \rho\zeta^k, \quad \forall \rho \in [-\infty, +\infty] \setminus \{0\}\}, \quad (2.16)$$

corresponding to process $\mathbf{y}^{k+1} = \tilde{\mathcal{F}}\mathbf{y}^k$, with $\tilde{\mathcal{F}} = \rho\mathcal{I} \circ \mathcal{F} \circ \frac{1}{\rho}\mathcal{I}$.

Proof. The proof follows straightforwardly from (2.12) and Lemma 2.2. \square

2.4.2 hidden step-size challenge

Given the above ρ -distanced parallel sequences, clearly, all of them share the same convergence properties, including rates and the best step-size choice. Then, we would determine such a best choice by optimizing the convergence rate.

A standard way to find a worst-case optimal step-size is to minimize an upper bound. However, with the above parallelism, there exists a hidden obstacle. To see this, consider the following convergence rate bounds (hold whenever \mathcal{F} is firmly non-expansive, see later Proposition 3.2):

$$\|\zeta^{k+1} - \zeta^k\|^2 \leq \frac{1}{k+1} \|\zeta^* - \zeta^0\|^2, \quad (2.17)$$

$$\|y^{k+1} - y^k\|^2 \leq \frac{1}{k+1} \|y^* - y^0\|^2. \quad (2.18)$$

The obstacle is that the above two upper bounds are different in general. If the ρ -distanced parallelism is not removed, then directly minimizing the upper bounds with respect to any ρ -related variable will lead to contradicted step-size choices in general.

As an example, recall from (1.11) the two fixed-point expressions in the current literature, restated here as

$$\zeta_1^* = \mathcal{A}x^* + \lambda^*/\gamma, \quad \zeta_2^* = \gamma\mathcal{A}x^* + \lambda^*, \quad (2.19)$$

which are related via $\zeta_2^* = \gamma\zeta_1^*$, leading to the following two optimization problems:

$$\underset{\gamma>0}{\text{minimize}} \quad \|\mathcal{A}x^* + \lambda^*/\gamma - \zeta_1^0\|^2, \quad (2.20)$$

$$\underset{\gamma>0}{\text{minimize}} \quad \|\gamma\mathcal{A}x^* + \lambda^* - \zeta_2^0\|^2, \quad (2.21)$$

which will yield different optimal solutions γ^* that are problematic, see more details in Sec. 4.1.1.

2.5 Unscaling guarantee

The key to our success is to guarantee no step-size related extra scaling exists when we optimize a convergence rate upper bound.

2.5.1 a conventional success

Before providing our solution, we briefly review a typical success in the literature, which implicitly avoided the above scaling issue.

Indeed, a natural way to address such an extra scaling is by division. Consider optimizing the following ratio:

$$\delta = \sup_{\{k|\zeta^{k+1} \neq \zeta^k\}} \frac{\|\zeta^{k+1} - \zeta^*\|}{\|\zeta^k - \zeta^*\|} = \sup_{\{k|y^{k+1} \neq y^k\}} \frac{\|y^{k+1} - y^*\|}{\|y^k - y^*\|}, \quad (2.22)$$

which holds for any non-zero ρ -distanced parallel sequences $y^k = \rho\zeta^k$. Such a ratio-factor optimizing approach is proposed in [25] for quadratic programming, and [26] for decentralized consensus problems. However, there are two notable drawbacks:

- (i) First, the factor δ needs to be the same for every iteration k , otherwise optimizing it only improves a few middle steps, and the whole convergence rate does not necessarily improve. This requirement can be satisfied when the convergence rate is linear. However, a linear rate does not hold in general (requires a strong assumption, see later Proposition 3.2). That said, the step-size choice obtained from here is not universally applicable.

- (ii) More importantly, their successes require analytical tractability, i.e., the fixed-point operator \mathcal{F} (equivalently, all algorithm iterates/sub-problems) admits an explicit analytical form. This requirement is not feasible for a large number of convex programs, which again limits its scope.

In view of these drawbacks, a general step-size selection scheme seems not attainable following this ratio-factor optimizing path.

2.5.2 idea sketch

A natural question is — apart from the above division approach, is there another way to guarantee no extra scaling?

The answer is affirmative, by appealing to symmetry. Given a certain fixed-point operator (an observation), suppose an extra scaling exists. Then, it can be characterized into

$$\mathcal{F}_{\text{obs}} = \rho \mathcal{I} \circ \mathcal{F}_0 \circ \frac{1}{\rho} \mathcal{I}, \quad \rho \neq 0, \quad (2.23)$$

where \mathcal{F}_0 denotes the underlying unscaled operator.

The insight is that the extra scaling structure $\rho \mathcal{I} \circ (\cdot) \circ \frac{1}{\rho} \mathcal{I}$ is not symmetric. Then, consider its adjoint operator $\mathcal{F}_{\text{obs}}^* : \mathbb{H} \rightarrow \mathbb{H}$, which can be abstractly written as

$$\mathcal{F}_{\text{obs}}^* = \left(\rho \mathcal{I} \circ \mathcal{F}_0 \circ \frac{1}{\rho} \mathcal{I} \right)^* = \frac{1}{\rho} \mathcal{I} \circ \mathcal{F}_0^* \circ \rho \mathcal{I}. \quad (2.24)$$

Compare (2.23) and (2.24), we see that the extra scaling structure changes. Now, suppose the following always holds for all choices of step-size parameter $\rho \neq 0$:

$$\mathcal{F}_{\text{obs}} = \mathcal{F}_{\text{obs}}^*, \quad (\text{to prove})$$

which clearly includes the case $\mathcal{F}_0 = \mathcal{F}_0^*$, since we assume it holds $\forall \rho \neq 0$.

Then, under this assumption, clearly we can conclude that \mathcal{F}_{obs} does not contain the extra scaling structure. Relation (to prove) will be concretely proved later in Sec. 2.8.2, and the proof relies on some properties of our domain parametrization, which we first establish them below.

2.6 Domain parametrization: useful properties

2.6.1 non-zero scalar parameter

Here, we show that the domain-parametrized proximal operator is well-defined.

Proposition 2.2. *The domain-parametrized proximal operator Prox_{f_ρ} defined in (2.5) is firmly nonexpansive and single-valued.*

Proof. To start, we need some lemmas.

Lemma 2.4. [27, Proposition 6.19] *Let C be a convex subset of \mathbb{H} , let \mathbb{K} be a real Hilbert space, let $\mathcal{L} \in \mathfrak{B}(\mathbb{H}, \mathbb{K})$ and let D be a convex subset of \mathbb{K} . Let $\text{int}(\cdot)$ and $\text{sri}(\cdot)$ denote the interior and the strong relative interior, respectively. Suppose $D \cap \text{int } \mathcal{L}(C) \neq \emptyset$ or $\mathcal{L}(C) \cap \text{int } D \neq \emptyset$. Then, $0 \in \text{sri}(D - \mathcal{L}(C))$.*

Lemma 2.5. [27, Corollary 16.53] *Let f be a CCP function and $\mathcal{L} \in \mathfrak{B}(\mathbb{H}, \mathbb{K})$. Suppose $0 \in \text{sri}(\text{dom}(f) - \text{ran}(\mathcal{L}))$. Then,*

$$\partial(f \circ \mathcal{L}) = \mathcal{L}^* \circ \partial f \circ \mathcal{L}.$$

Lemma 2.6. [27, Proposition 23.25] *Let \mathbb{K} be a real Hilbert space, suppose $\mathcal{L} \in \mathfrak{B}(\mathbb{H}, \mathbb{K})$ is such that $\mathcal{L}\mathcal{L}^*$ is invertible, let $\mathcal{A} : \mathbb{K} \rightarrow 2^{\mathbb{K}}$ be maximal monotone, and set $\mathcal{B} = \mathcal{L}^*\mathcal{A}\mathcal{L}$. Then, $\mathcal{B} : \mathbb{H} \rightarrow 2^{\mathbb{H}}$ is maximal monotone.*

For the above 3 lemmas, substitute the mapping \mathcal{L} there with our scalar one $\rho\mathcal{I}$ ($\rho \neq 0$). First, a non-zero scaling is clearly bijective, the two spaces in the above lemmas hence coincide, i.e., $\mathbb{H} = \mathbb{K}$. Moreover, the range of a non-zero scalar map is clearly the entire Hilbert space, i.e., $\text{ran}(\rho\mathcal{I}) = \mathbb{K} = \mathbb{H}$.

In view of Lemma 2.4, substitute the set \mathcal{D} there with $\text{dom}(f)$ (subset of \mathbb{H}). Then, $\text{ran}(\rho\mathcal{I}) \cap \text{int } \text{dom}(f) = \mathbb{H} \cap \text{int } \text{dom}(f) \neq \emptyset$, which holds unless $\text{dom}(f) = \emptyset$ (omitted by assumption). Therefore, we arrive at $0 \in \text{sri}(\text{dom}(f) - \text{ran}(\rho\mathcal{I}))$.

Then, invoke Lemma 2.5, we have $\partial(f\rho) = \rho\mathcal{I} \circ (\partial f) \circ \rho\mathcal{I}$. By Lemma 2.6, the operator $\partial(f\rho)$ is maximal monotone.

Now, invoke definition (2.5),

$$\begin{aligned} \text{Prox}_{f\rho}(\mathbf{v}) &= \underset{\mathbf{z}}{\text{argmin}} \ f(\rho\mathbf{z}) + \frac{1}{2}\|\mathbf{z} - \mathbf{v}\|^2 \iff \mathbf{v} - \mathbf{z} \in \partial(f\rho)(\mathbf{z}), \\ &\iff \mathbf{z} = (\mathcal{I} + \partial(f\rho))^{-1}(\mathbf{v}). \end{aligned} \quad (2.25)$$

Owing to $\partial(f\rho)$ being maximal monotone, the proximal operator is single-valued and firmly nonexpansive, see e.g. [27]. The proof is now concluded. \square

2.6.2 injective operator parameter

Here, we show that an injective parameter is feasible in two special cases. This aspect enables some simple, unified analysis frameworks for ADMM and primal-dual problems in the next sections.

Proposition 2.3. [single-valued] *Given $f \in \Gamma_0(\mathbb{H})$, $\text{dom}(f) \neq \emptyset$ and $\mathcal{D} \in \mathfrak{B}(\mathbb{H}, \mathbb{K})$ being injective. Let $\mathcal{D}^* \in \mathfrak{B}(\mathbb{K}, \mathbb{H})$ and $\mathcal{D}^{-1} \in \mathfrak{B}(\mathbb{K}, \mathbb{H})$ denote the adjoint and inverse mappings, respectively. Then, the following proximal operators are firmly non-expansive and single-valued:*

$$\text{Prox}_{f\mathcal{D}^{-1}}(\mathbf{v}) = \underset{\mathbf{z}_1 \in \mathbb{K}}{\text{argmin}} \ f(\mathcal{D}^{-1}\mathbf{z}_1) + \frac{1}{2}\|\mathbf{z}_1 - \mathbf{v}\|^2, \quad (2.26)$$

$$\text{Prox}_{f\mathcal{D}^*}(\mathbf{v}) = \underset{\mathbf{z}_1 \in \mathbb{K}}{\text{argmin}} \ f(\mathcal{D}^*\mathbf{z}_1) + \frac{1}{2}\|\mathbf{z}_1 - \mathbf{v}\|^2. \quad (2.27)$$

Proof. The proof follows similar procedures as Proposition 2.2, with different substitutions. We will invoke the same lemmas and substitute the mapping \mathcal{L} there with \mathcal{D}^{-1} and \mathcal{D}^* . To avoid repeating, below we no longer state such lemmas.

For both cases, $\mathcal{L} = \mathcal{D}^{-1}$ and $\mathcal{L} = \mathcal{D}^*$, we always have $\text{ran}(\mathcal{L}) = \text{dom } \mathcal{D} = \mathbb{H}$. It follows that $\text{ran}(\mathcal{L}) \cap \text{int dom}(f) = \mathbb{H} \cap \text{int dom}(f) \neq \emptyset$, which holds unless $\text{dom}(f) = \emptyset$ (omitted by assumption).

Now, invoke Lemma 2.5, we have $\partial(f \circ \mathcal{L}) = \mathcal{L}^*(\partial f) \mathcal{L}$. All what left is regarding Lemma 2.6, where we need $\mathcal{L}\mathcal{L}^*$ there being invertible. Let $\mathcal{L} = \mathcal{D}^{-1}$, then

$$\mathcal{L}\mathcal{L}^* = \mathcal{D}^{-1}(\mathcal{D}^*)^{-1} = (\mathcal{D}^*\mathcal{D})^{-1}, \quad (2.28)$$

Let $\mathcal{L} = \mathcal{D}^*$, then

$$\mathcal{L}\mathcal{L}^* = \mathcal{D}^*(\mathcal{D}^*)^* = \mathcal{D}^*\mathcal{D}. \quad (2.29)$$

Since \mathcal{D} is assumed injective, the above two cases are clearly both invertible. The proof is therefore concluded. \square

Next, we establish some alternative/equivalent characterizations for the above $\mathbf{Prox}_{f\mathcal{D}^{-1}}$ and $\mathbf{Prox}_{f\mathcal{D}^*}$, which will be used later. To start, we need some lemmas.

Definition 2.4. *The orthogonal complement of a subset C of \mathbb{H} is: $C^\perp = \{\mathbf{x} \in \mathbb{H} \mid \langle \mathbf{x}, \mathbf{y} \rangle = 0, \forall \mathbf{y} \in C\}$.*

Lemma 2.7. *[27, Fact 2.25] Let $\mathcal{T} \in \mathfrak{B}(\mathbb{H}, \mathbb{K})$, and let $\ker \mathcal{T} = \{\mathbf{x} \in \mathbb{H} \mid \mathcal{T}\mathbf{x} = \mathbf{0}\}$ be the kernel of \mathcal{T} . Then, $\ker \mathcal{T}^* = (\text{ran } \mathcal{T})^\perp$.*

Lemma 2.8. *Let $\mathcal{D} \in \mathfrak{B}(\mathbb{H}, \mathbb{K})$ be injective. Then, its adjoint inverse mapping $(\mathcal{D}^*)^{-1} : \mathbb{H} \rightarrow \mathbb{K}$ is also injective.*

Proof. First, let us note that

$$\text{ran } \mathcal{D}^{-1} = \text{dom } \mathcal{D} = \mathbb{H}. \quad (2.30)$$

Then, by Definition 2.4, we obtain

$$(\text{ran } \mathcal{D}^{-1})^\perp = (\text{dom } \mathcal{D})^\perp = \{\mathbf{x} \in \mathbb{H} \mid \langle \mathbf{x}, \mathbf{y} \rangle = 0, \forall \mathbf{y} \in \text{dom } \mathcal{D} = \mathbb{H}\}. \quad (2.31)$$

Since the above defined \mathbf{y} takes value in the entire space \mathbb{H} , the above set clearly only contains the zero vector, i.e.,

$$(\text{ran } \mathcal{D}^{-1})^\perp = \{\mathbf{0}\}. \quad (2.32)$$

By Lemma 2.7, the above implies

$$\ker (\mathcal{D}^*)^{-1} = (\text{ran } \mathcal{D}^{-1})^\perp = \{\mathbf{0}\}. \quad (2.33)$$

That implies $(\mathcal{D}^*)^{-1}$ being injective, which concludes the proof. \square

Lemma 2.9 (transformation). *Given $f \in \Gamma_0(\mathbb{H})$, $\text{dom}(f) \neq \emptyset$ and $\mathcal{D} \in \mathfrak{B}(\mathbb{H}, \mathbb{K})$ being injective. Then,*

$$\begin{aligned} \mathcal{D} \underset{\mathbf{z}_2 \in \mathbb{H}}{\text{argmin}} f(\mathbf{z}_2) + \frac{1}{2} \|\mathcal{D}\mathbf{z}_2 - \mathbf{v}\|^2 &= \underbrace{\underset{\mathbf{z}_1 \in \mathbb{K}}{\text{argmin}} f(\mathcal{D}^{-1}\mathbf{z}_1) + \frac{1}{2} \|\mathbf{z}_1 - \mathbf{v}\|^2}_{\mathbf{Prox}_{f\mathcal{D}^{-1}}(\mathbf{v})}, \\ (\mathcal{D}^*)^{-1} \underset{\mathbf{z}_2 \in \mathbb{H}}{\text{argmin}} f(\mathbf{z}_2) + \frac{1}{2} \|(\mathcal{D}^*)^{-1}\mathbf{z}_2 - \mathbf{v}\|^2 &= \underbrace{\underset{\mathbf{z}_1 \in \mathbb{K}}{\text{argmin}} f(\mathcal{D}^*\mathbf{z}_1) + \frac{1}{2} \|\mathbf{z}_1 - \mathbf{v}\|^2}_{\mathbf{Prox}_{f\mathcal{D}^*}(\mathbf{v})}. \end{aligned}$$

Proof. The proof is straightforward by a variable substitution.

For the first relation, we prove from its left-hand-side. Let $\mathbf{z}_1 = \mathcal{D}\mathbf{z}_2$, which is a one-to-one correspondence, owing to \mathcal{D} being injective. Hence, we obtain

$$\operatorname{argmin}_{\mathbf{z}_2 \in \mathbb{H}} f(\mathbf{z}_2) + \frac{1}{2} \|\mathcal{D}\mathbf{z}_2 - \mathbf{v}\|^2 = \operatorname{argmin}_{(\mathcal{D}^{-1}\mathbf{z}_1) \in \mathbb{H}} f(\mathcal{D}^{-1}\mathbf{z}_1) + \frac{1}{2} \|\mathbf{z}_1 - \mathbf{v}\|^2, \quad (2.34)$$

which yields a minimizer relation $\mathbf{z}_2^* = \mathcal{D}^{-1}\mathbf{z}_1^*$, which can be rewritten into $\mathcal{D}\mathbf{z}_2^* = \mathbf{z}_1^*$. This gives the first relation above.

Same arguments hold for the second case, where mapping $(\mathcal{D}^*)^{-1}$ is injective by Lemma 2.8. We omit the same arguments to avoid repeating. The proof is now concluded. \square

Lemma 2.10 (single-valued partial evaluation). *Given $f \in \Gamma_0(\mathbb{H})$ and $\operatorname{dom}(f) \neq \emptyset$. Let $\mathcal{D} \in \mathfrak{B}(\mathbb{H}, \mathbb{K})$ be injective. Then, the following two evaluations are single-valued:*

$$\operatorname{argmin}_{\mathbf{z}_2 \in \mathbb{H}} f(\mathbf{z}_2) + \frac{1}{2} \|\mathcal{D}\mathbf{z}_2 - \mathbf{v}\|^2, \quad (2.35)$$

$$\operatorname{argmin}_{\mathbf{z}_2 \in \mathbb{H}} f(\mathbf{z}_2) + \frac{1}{2} \|(\mathcal{D}^*)^{-1}\mathbf{z}_2 - \mathbf{v}\|^2, \quad (2.36)$$

or equivalently, the following two mappings are single-valued:

$$(\mathcal{D}^*\mathcal{D} + \partial f)^{-1}\mathcal{D}^*, \quad ((\mathcal{D}^*\mathcal{D})^{-1} + \partial f)^{-1}\mathcal{D}^{-1}. \quad (2.37)$$

Proof. Following from Lemma 2.9,

$$\underbrace{\mathcal{D} \operatorname{argmin}_{\mathbf{z}_2 \in \mathbb{H}} f(\mathbf{z}_2) + \frac{1}{2} \|\mathcal{D}\mathbf{z}_2 - \mathbf{v}\|^2}_{(2.35)} = \mathbf{Prox}_{f\mathcal{D}^{-1}}(\mathbf{v}), \quad (2.38)$$

where the right-hand side is single-valued by Proposition 2.3. Since \mathcal{D} is assumed injective, i.e., a one-to-one correspondence, then its domain element, corresponding to (2.35), has to be single-valued.

Same arguments hold for the symmetric case (2.36) and is omitted to avoid repeating. The expressions in (2.37) follows instantly by the first-order optimality condition. The proof is now concluded. \square

2.6.3 Domain-parametrized Moreau identity

Proposition 2.4. *Given $f \in \Gamma_0(\mathbb{H})$ and $\operatorname{dom}(f) \neq \emptyset$. Let $\mathcal{D} \in \mathfrak{B}(\mathbb{H}, \mathbb{K})$ be injective. Then, the following relation holds:*

$$\mathbf{v} = \mathbf{Prox}_{f\mathcal{D}^{-1}}(\mathbf{v}) + \mathbf{Prox}_{f^*\mathcal{D}^*}(\mathbf{v}), \quad \forall \mathbf{v} \in \mathbb{K}. \quad (2.39)$$

Proof. First, by Proposition 2.3, the above $\mathbf{Prox}_{f\mathcal{D}^{-1}}$ and $\mathbf{Prox}_{f^*\mathcal{D}^*}$ are well-defined. Now, let

$$\mathbf{x}^* = \operatorname{argmin}_{\mathbf{x}} f(\mathbf{x}) + \frac{1}{2} \|\mathcal{D}\mathbf{x} - \mathbf{v}\|^2, \quad (2.40)$$

$$\mathbf{y}^* = \operatorname{argmin}_{\mathbf{y}} f^*(\mathbf{y}) + \frac{1}{2} \|(\mathcal{D}^*)^{-1}\mathbf{y} - \mathbf{v}\|^2, \quad (2.41)$$

which are both single-valued by Lemma 2.10. By Lemma 2.9, our goal can be converted to proving the following relation:

$$\mathbf{v} = \mathcal{D}\mathbf{x}^* + (\mathcal{D}^*)^{-1}\mathbf{y}^* \iff \mathbf{y}^* = \mathcal{D}^*(\mathbf{v} - \mathcal{D}\mathbf{x}^*). \quad (\text{goal})$$

To this end, consider \mathbf{x}^* first. Invoke the first-order optimality condition for (2.40), we obtain

$$\mathcal{D}^*\mathbf{v} - \mathcal{D}^*\mathcal{D}\mathbf{x}^* \in \partial f(\mathbf{x}^*), \quad (2.42)$$

$$\iff \mathbf{x}^* \in \partial f^*(\mathcal{D}^*\mathbf{v} - \mathcal{D}^*\mathcal{D}\mathbf{x}^*), \quad (2.43)$$

$$\iff \mathcal{D}^{-1}(\mathbf{v} - \mathbf{v} + \mathcal{D}\mathbf{x}^*) \in \partial f^*(\mathcal{D}^*\mathbf{v} - \mathcal{D}^*\mathcal{D}\mathbf{x}^*), \quad (2.44)$$

$$\iff \mathcal{D}^{-1}(\mathbf{v} - (\mathcal{D}^*)^{-1} \underbrace{\mathcal{D}^*(\mathbf{v} - \mathcal{D}\mathbf{x}^*)}_{\stackrel{\text{def}}{=} \mathbf{t}}) \in \partial f^*(\underbrace{\mathcal{D}^*\mathbf{v} - \mathcal{D}^*\mathcal{D}\mathbf{x}^*}_{\stackrel{\text{def}}{=} \mathbf{t}}), \quad (2.45)$$

$$\iff \mathcal{D}^{-1}(\mathbf{v} - (\mathcal{D}^*)^{-1}\mathbf{t}) \in \partial f^*(\mathbf{t}), \quad (2.46)$$

$$\iff \mathbf{t} = ((\mathcal{D}^*\mathcal{D})^{-1} + \partial f^*)^{-1}\mathcal{D}^{-1}(\mathbf{v}), \quad (2.47)$$

with the last line equality owes to the single-valued property, recall Lemma 2.10, where $\mathbf{t} \stackrel{\text{def}}{=} \mathcal{D}^*(\mathbf{v} - \mathcal{D}\mathbf{x}^*)$ is a variable substitution.

Now, consider \mathbf{y}^* . Invoke the first-order optimality condition for (2.41), we obtain

$$\mathcal{D}^{-1}(\mathbf{v} - (\mathcal{D}^*)^{-1}\mathbf{y}^*) \in \partial f^*(\mathbf{y}^*), \quad (2.48)$$

$$\iff \mathbf{y}^* = ((\mathcal{D}^*\mathcal{D})^{-1} + \partial f^*)^{-1}\mathcal{D}^{-1}(\mathbf{v}), \quad (2.49)$$

with the last line equality owing to the single-valued property, recall Lemma 2.10.

Compare (2.47) and (2.49), the expressions are exactly the same. That is,

$$\mathbf{y}^* = \mathbf{t} = \mathcal{D}^*(\mathbf{v} - \mathcal{D}\mathbf{x}^*), \quad (2.50)$$

which proves (goal). The proof is now concluded. \square

2.7 Domain-parametrized ADMM

Here, we express the ADMM algorithm in terms of our domain-parametrized proximal operator. We see some useful new results, particularly, a great analysis convenience.

Consider a general convex problem:

$$\begin{aligned} & \underset{\mathbf{x}, \mathbf{z}}{\text{minimize}} && f(\mathbf{x}) + g(\mathbf{z}), \\ & \text{subject to} && \mathcal{A}\mathbf{x} - \mathcal{B}\mathbf{z} = \mathbf{c}, \end{aligned} \quad (\text{problem})$$

with variables $\mathbf{x} \in \mathbb{H}$, $\mathbf{z} \in \mathbb{P}$, $\mathbf{c} \in \mathbb{K}$ and functions $f \in \Gamma_0(\mathbb{H})$, $g \in \Gamma_0(\mathbb{P})$, where $\mathcal{A} \in \mathfrak{B}(\mathbb{H}, \mathbb{K})$ and $\mathcal{B} \in \mathfrak{B}(\mathbb{P}, \mathbb{K})$ are injective. We assume a solution always exists.

The augmented Lagrangian can be written as

$$\mathcal{L}_\rho(\mathbf{x}, \mathbf{z}, \boldsymbol{\lambda}) = f(\mathbf{x}) + g(\mathbf{z}) + \frac{1}{2}\|\rho(\mathcal{A}\mathbf{x} - \mathcal{B}\mathbf{z} - \mathbf{c}) + \boldsymbol{\lambda}/\rho\|^2, \quad (2.51)$$

where $\rho \neq 0$ is a non-zero step-size parameter. The ADMM iterates are

$$\begin{aligned} \mathbf{x}^{k+1} &= \underset{\mathbf{x} \in \mathbb{H}}{\operatorname{argmin}} f(\mathbf{x}) + \frac{1}{2} \|\rho(\mathcal{A}\mathbf{x} - \mathcal{B}\mathbf{z}^k - \mathbf{c}) + \boldsymbol{\lambda}^k / \rho\|^2, \\ \mathbf{z}^{k+1} &= \underset{\mathbf{z} \in \mathbb{P}}{\operatorname{argmin}} g(\mathbf{z}) + \frac{1}{2} \|\rho(\mathcal{A}\mathbf{x}^{k+1} - \mathcal{B}\mathbf{z} - \mathbf{c}) + \boldsymbol{\lambda}^k / \rho\|^2, \\ \boldsymbol{\lambda}^{k+1} &= \boldsymbol{\lambda}^k + \rho^2(\mathcal{A}\mathbf{x}^{k+1} - \mathcal{B}\mathbf{z}^{k+1} - \mathbf{c}). \end{aligned} \quad (2.52)$$

2.7.1 New proximal steps

Given $\mathcal{A} \in \mathfrak{B}(\mathbb{H}, \mathbb{K})$ and $\mathcal{B} \in \mathfrak{B}(\mathbb{P}, \mathbb{K})$ being injective. Clearly, $\rho\mathcal{A}$ and $\rho\mathcal{B}$ are also injective $\forall \rho \neq 0$, and therefore both the inverse and the adjoint mappings are well-defined parameters by Proposition 2.3.

Then, by Lemma 2.9, we can rewrite the ADMM iterates into:

$$\begin{aligned} \rho\mathcal{A}\mathbf{x}^{k+1} &= \mathbf{Prox}_{f(\rho\mathcal{A})^{-1}} \left(\rho\mathbf{c} + \rho\mathcal{B}\mathbf{z}^k - \boldsymbol{\lambda}^k / \rho \right), \\ \rho\mathcal{B}\mathbf{z}^{k+1} &= \mathbf{Prox}_{g(\rho\mathcal{B})^{-1}} \left(-\rho\mathbf{c} + \rho\mathcal{A}\mathbf{x}^{k+1} + \boldsymbol{\lambda}^k / \rho \right), \\ \boldsymbol{\lambda}^{k+1} &= \boldsymbol{\lambda}^k + \rho^2(\mathcal{A}\mathbf{x}^{k+1} - \mathcal{B}\mathbf{z}^{k+1} - \mathbf{c}). \end{aligned} \quad (\text{prox. ADMM})$$

We may further simplify the above via the following variable substitutions:

$$\tilde{\mathbf{x}}^k \stackrel{\text{def}}{=} \rho\mathcal{A}\mathbf{x}^k, \quad \tilde{\mathbf{z}}^k \stackrel{\text{def}}{=} \rho\mathcal{B}\mathbf{z}^k, \quad \tilde{\boldsymbol{\lambda}}^k \stackrel{\text{def}}{=} \frac{1}{\rho}\boldsymbol{\lambda}^k, \quad \tilde{\mathbf{c}} \stackrel{\text{def}}{=} \rho\mathbf{c}. \quad (2.53)$$

This leads to the following *scaled form*:

$$\begin{aligned} \tilde{\mathbf{x}}^{k+1} &= \mathbf{Prox}_{f(\rho\mathcal{A})^{-1}} \left(\tilde{\mathbf{c}} + \tilde{\mathbf{z}}^k - \tilde{\boldsymbol{\lambda}}^k \right), \\ \tilde{\mathbf{z}}^{k+1} &= \mathbf{Prox}_{g(\rho\mathcal{B})^{-1}} \left(-\tilde{\mathbf{c}} + \tilde{\mathbf{x}}^{k+1} + \tilde{\boldsymbol{\lambda}}^k \right), \\ \tilde{\boldsymbol{\lambda}}^{k+1} &= \tilde{\boldsymbol{\lambda}}^k + \tilde{\mathbf{x}}^{k+1} - \tilde{\mathbf{z}}^{k+1} - \tilde{\mathbf{c}}. \end{aligned} \quad (\text{scaled form})$$

Remarks 2.3 (enabled proximal steps). To our knowledge, the above proximal expression is not available in the current literature (regarding the general constrained form (problem)), see comments from Radu Ioan Bot and Erno Robert Csetnek [28]: ‘*Generally, the minimization with respect to the variable x does not lead to a proximal step*’, with workarounds on this issue in e.g. [29, 30].

2.7.2 Convergence: a direct establishment

In the literature, a typical way to establish the ADMM convergence for the general form (problem) is by first converting to an unconstrained form, either via an *infimal post-composition* [9, sec. 3.1], or dualization [9, sec. 3.2], [22]. Then, convergence is shown via the Douglas-Rachford splitting (DRS) iterates.

Here, owing to the direct proximal steps (scaled form), we are able to establish a direct characterization (no conversion to DRS). To start, we need two lemmas.

Lemma 2.11. *Let $h(\mathbf{z}) = f(\mathbf{z}) - \langle \mathbf{c}, \mathbf{z} \rangle$. Then,*

$$\mathbf{Prox}_{h\rho^{-1}}(\mathbf{v}) = \mathbf{Prox}_{f\rho^{-1}}(\mathbf{c} + \mathbf{v}). \quad (2.54)$$

Proof. The proof follows straightforwardly from definition:

$$\begin{aligned} \mathbf{Prox}_{h\rho^{-1}}(\mathbf{v}) &= \underset{\mathbf{z}_1}{\operatorname{argmin}} h(\rho^{-1}\mathbf{z}_1) + \frac{1}{2}\|\mathbf{z}_1 - \mathbf{v}\|^2 \\ &= \underset{\mathbf{z}_1}{\operatorname{argmin}} f(\rho^{-1}\mathbf{z}_1) - \langle \mathbf{c}, \mathbf{z}_1 \rangle + \frac{1}{2}\|\mathbf{z}_1 - \mathbf{v}\|^2 \\ &= \underset{\mathbf{z}_1}{\operatorname{argmin}} f(\rho^{-1}\mathbf{z}_1) + \frac{1}{2}\|\mathbf{z}_1 - \mathbf{c} - \mathbf{v}\|^2 \\ &= \mathbf{Prox}_{f\rho^{-1}}(\mathbf{c} + \mathbf{v}), \end{aligned} \quad (2.55)$$

which concludes the proof. \square

Lemma 2.12 (1/2-averaging, see e.g. [9, 27]). *Let $\mathcal{T} : \mathbb{H} \rightarrow \mathbb{H}$ be non-expansive. Then, the 1/2-averaging $\frac{1}{2}\mathcal{I} + \frac{1}{2}\mathcal{T}$ is firmly non-expansive. Reversely, let $\mathcal{F} : \mathbb{H} \rightarrow \mathbb{H}$ be firmly non-expansive, then $2\mathcal{F} - \mathcal{I}$ is non-expansive.*

Now, we are in position to establish the convergence.

Proposition 2.5 (convergence). *(prox. ADMM) and (scaled form) admit the following fixed-point characterization:*

$$\boldsymbol{\zeta}^{k+1} = \mathcal{F}_{ADMM} \boldsymbol{\zeta}^k, \quad (2.56)$$

with $\boldsymbol{\zeta}^{k+1} = \rho\mathcal{A}\mathbf{x}^{k+1} + \frac{1}{\rho}\boldsymbol{\lambda}^k$, where

$$\mathcal{F}_{ADMM} = \frac{1}{2}(2\mathbf{Prox}_{\bar{f}} - \mathcal{I}) \circ (2\mathbf{Prox}_{\hat{g}} - \mathcal{I}) + \frac{1}{2}\mathcal{I},$$

and where

$$\bar{f}(\mathbf{y}) \stackrel{\text{def}}{=} f \circ (\rho\mathcal{A})^{-1}(\mathbf{y}) - \langle \rho\mathbf{c}, \mathbf{y} \rangle, \quad (2.57)$$

$$\hat{g}(\mathbf{y}) \stackrel{\text{def}}{=} g \circ (\rho\mathcal{B})^{-1}(\mathbf{y}) + \langle \rho\mathbf{c}, \mathbf{y} \rangle, \quad \forall \mathbf{y} \in \mathbb{K}. \quad (2.58)$$

The sequence $\{\boldsymbol{\zeta}^k\}$ converges to a fixed-point $\boldsymbol{\zeta}^* \in \text{Fix } \mathcal{F}_{ADMM}$ (if it exists).

Proof. For light of notations, we prove via the (scaled form), with substitutions restated here as:

$$\tilde{\mathbf{x}}^k \stackrel{\text{def}}{=} \rho\mathcal{A}\mathbf{x}^k, \quad \tilde{\mathbf{z}}^k \stackrel{\text{def}}{=} \rho\mathcal{B}\mathbf{z}^k, \quad \tilde{\boldsymbol{\lambda}}^k \stackrel{\text{def}}{=} \frac{1}{\rho}\boldsymbol{\lambda}^k, \quad \tilde{\mathbf{c}} \stackrel{\text{def}}{=} \rho\mathbf{c}. \quad (2.59)$$

In view of the $\boldsymbol{\lambda}$ -update in (scaled form), we have

$$\tilde{\boldsymbol{\lambda}}^k = \tilde{\boldsymbol{\lambda}}^{k-1} + \tilde{\mathbf{x}}^k - \tilde{\mathbf{z}}^k - \tilde{\mathbf{c}} = \boldsymbol{\zeta}^k - \tilde{\mathbf{z}}^k - \tilde{\mathbf{c}}. \quad (2.60)$$

Then, we arrive at

$$\begin{aligned}
\zeta^{k+1} &= \tilde{x}^{k+1} + \tilde{\lambda}^k, \\
&= \mathbf{Prox}_{f(\rho\mathcal{A})^{-1}}(2\tilde{c} + 2\tilde{z}^k - \zeta^k) + \zeta^k - \tilde{z}^k - \tilde{c}, \\
&= \mathbf{Prox}_{f(\rho\mathcal{A})^{-1}}\left(\tilde{c} + 2\mathbf{Prox}_{g(\rho\mathcal{B})^{-1}}(\zeta^k - \tilde{c}) - (\zeta^k - \tilde{c})\right) + \\
&\quad (\zeta^k - \tilde{c}) - \mathbf{Prox}_{g(\rho\mathcal{B})^{-1}}(\zeta^k - \tilde{c}), \\
&= \mathbf{Prox}_{f(\rho\mathcal{A})^{-1}} \circ \left(\tilde{c} + (2\mathbf{Prox}_{g(\rho\mathcal{B})^{-1}} - \mathcal{I})(\zeta^k - \tilde{c})\right) - \\
&\quad \frac{1}{2}\left(\tilde{c} + (2\mathbf{Prox}_{g(\rho\mathcal{B})^{-1}} - \mathcal{I})(\zeta^k - \tilde{c})\right) + \frac{1}{2}\zeta^k, \\
&= \underbrace{\left(\frac{1}{2}(2\mathbf{Prox}_{\bar{f}} - \mathcal{I}) \circ (2\mathbf{Prox}_{\hat{g}} - \mathcal{I}) + \frac{1}{2}\mathcal{I}\right)}_{\mathcal{F}_{ADMM}} \zeta^k,
\end{aligned} \tag{2.61}$$

where the last line uses Lemma 2.11 and substitutions:

$$\bar{f}(\mathbf{y}) \stackrel{\text{def}}{=} f \circ (\rho\mathcal{A})^{-1}(\mathbf{y}) - \langle \rho\mathbf{c}, \mathbf{y} \rangle, \tag{2.62}$$

$$\hat{g}(\mathbf{y}) \stackrel{\text{def}}{=} g \circ (\rho\mathcal{B})^{-1}(\mathbf{y}) + \langle \rho\mathbf{c}, \mathbf{y} \rangle, \quad \forall \mathbf{y} \in \mathbb{K}. \tag{2.63}$$

By Lemma 2.12, the above \mathcal{F}_{ADMM} is firmly non-expansive. It follows that sequence $\{\zeta^k\}$ converges to a fixed-point $\zeta^* \in \text{Fix } \mathcal{F}_{ADMM}$ (if it exists), see e.g. [27, 22].

At last, invoke definition (2.59), we obtain the expression:

$$\zeta^{k+1} = \tilde{x}^{k+1} + \tilde{\lambda}^k = \rho\mathcal{A}x^{k+1} + \frac{1}{\rho}\lambda^k. \tag{2.64}$$

The proof is now concluded. \square

2.8 Duality

Here, we consider the dual characterization, which is key to establishing the above fixed-point expression (2.64) being unscaled, corresponding to Sec. 2.5.2.

2.8.1 Domain-parametrized primal-dual characterization

Here, we dualize (problem), restated here as (primal problem):

$$\begin{aligned}
&\underset{\mathbf{x}, \mathbf{z}}{\text{minimize}} && f(\mathbf{x}) + g(\mathbf{z}), \\
&\text{subject to} && \mathcal{A}\mathbf{x} - \mathcal{B}\mathbf{z} = \mathbf{c},
\end{aligned} \tag{2.65}$$

with variables $\mathbf{x} \in \mathbb{H}$, $\mathbf{z} \in \mathbb{P}$, $\mathbf{c} \in \mathbb{K}$ and functions $f \in \Gamma_0(\mathbb{H})$, $g \in \Gamma_0(\mathbb{P})$, where $\mathcal{A} \in \mathfrak{B}(\mathbb{H}, \mathbb{K})$ and $\mathcal{B} \in \mathfrak{B}(\mathbb{P}, \mathbb{K})$ are injective. We assume a solution always exists.

To start, we need one lemma.

Lemma 2.13. *Given function $g \in \Gamma_0(\mathbb{H})$, let $h(\cdot) = g(\cdot) + \langle \mathbf{c}, \cdot \rangle$. Then,*

$$h^*(\cdot) = g^*(\cdot - \mathbf{c}). \tag{2.66}$$

Proof. By the Fenchel conjugate definition,

$$h^*(\mathbf{v}) = \sup_{\mathbf{z}} \langle \mathbf{z}, \mathbf{v} \rangle - g(\mathbf{z}) - \langle \mathbf{c}, \mathbf{z} \rangle = \sup_{\mathbf{z}} \langle \mathbf{z}, \mathbf{v} - \mathbf{c} \rangle - g(\mathbf{z}) = g^*(\mathbf{v} - \mathbf{c}), \quad (2.67)$$

which concludes the proof. \square

Proposition 2.6. *The convex program (2.65) admits the following primal-dual characterization:*

$$\underset{\tilde{\mathbf{x}}}{\text{minimize}} \quad \bar{f}(\tilde{\mathbf{x}}) + \hat{g}(\tilde{\mathbf{x}} - \tilde{\mathbf{c}}), \quad (\text{primal})$$

$$\underset{\tilde{\boldsymbol{\lambda}}}{\text{minimize}} \quad \bar{f}^* \circ (-\mathcal{I})(\tilde{\boldsymbol{\lambda}}) + \hat{g}^*(\tilde{\boldsymbol{\lambda}} - \tilde{\mathbf{c}}), \quad (\text{dual})$$

with variable defined as:

$$\tilde{\mathbf{x}} \stackrel{\text{def}}{=} \rho \mathcal{A} \mathbf{x} \in \mathbb{K}, \quad \tilde{\boldsymbol{\lambda}} \stackrel{\text{def}}{=} \boldsymbol{\lambda} / \rho \in \mathbb{K}, \quad \tilde{\mathbf{c}} \stackrel{\text{def}}{=} \rho \mathbf{c} \in \mathbb{K}, \quad (2.68)$$

and function defined as:

$$\bar{f}(\mathbf{y}) \stackrel{\text{def}}{=} f \circ (\rho \mathcal{A})^{-1}(\mathbf{y}) - \langle \rho \mathbf{c}, \mathbf{y} \rangle, \quad (2.69)$$

$$\hat{g}(\mathbf{y}) \stackrel{\text{def}}{=} g \circ (\rho \mathcal{B})^{-1}(\mathbf{y}) + \langle \rho \mathbf{c}, \mathbf{y} \rangle, \quad \forall \mathbf{y} \in \mathbb{K}. \quad (2.70)$$

Proof. Problem (problem) can be rewritten into

$$\begin{aligned} & \underset{\mathbf{x}, \mathbf{z}}{\text{minimize}} \quad f(\mathbf{x}) + g(\mathbf{z}) && \text{subject to } \mathcal{A}\mathbf{x} - \mathcal{B}\mathbf{z} = \mathbf{c}, \\ \iff & \underset{\mathbf{x}, \mathbf{z}}{\text{minimize}} \quad f(\rho \mathcal{A})^{-1}(\rho \mathcal{A}\mathbf{x}) + g(\rho \mathcal{B})^{-1}(\rho \mathcal{B}\mathbf{z}) && \text{subject to } \rho \mathcal{A}\mathbf{x} - \rho \mathcal{B}\mathbf{z} = \rho \mathbf{c}, \\ \iff & \underset{\tilde{\mathbf{x}}, \tilde{\mathbf{z}}}{\text{minimize}} \quad f(\rho \mathcal{A})^{-1}(\tilde{\mathbf{x}}) + g(\rho \mathcal{B})^{-1}(\tilde{\mathbf{z}}) - \|\tilde{\mathbf{c}}\|^2 && \text{subject to } \tilde{\mathbf{x}} - \tilde{\mathbf{z}} = \tilde{\mathbf{c}}, \\ \iff & \underset{\tilde{\mathbf{x}}, \tilde{\mathbf{z}}}{\text{minimize}} \quad \bar{f}(\tilde{\mathbf{x}}) + \hat{g}(\tilde{\mathbf{z}}) && \text{subject to } \tilde{\mathbf{x}} - \tilde{\mathbf{z}} = \tilde{\mathbf{c}}. \end{aligned}$$

with variable defined as: $\tilde{\mathbf{x}} = \rho \mathcal{A} \mathbf{x}$, $\tilde{\boldsymbol{\lambda}} = \boldsymbol{\lambda} / \rho$, $\tilde{\mathbf{c}} = \rho \mathbf{c}$, and function defined as: $\bar{f}(\mathbf{x}) = f \circ (\rho \mathcal{A})^{-1}(\mathbf{x}) - \langle \rho \mathbf{c}, \mathbf{x} \rangle$, $\hat{g}(\mathbf{x}) = g \circ (\rho \mathcal{B})^{-1}(\mathbf{x}) + \langle \rho \mathbf{c}, \mathbf{x} \rangle$.

Next, we derive the dual problem. Consider the following Lagrangian:

$$\begin{aligned} \mathcal{L}(\mathbf{x}, \mathbf{z}, \boldsymbol{\lambda}) &= f(\mathbf{x}) + g(\mathbf{z}) + \langle \boldsymbol{\lambda}, \mathcal{A}\mathbf{x} - \mathcal{B}\mathbf{z} - \mathbf{c} \rangle, \\ &= f(\mathbf{x}) + g(\mathbf{z}) + \langle (\rho)^{-1} \boldsymbol{\lambda}, \rho(\mathcal{A}\mathbf{x} - \mathcal{B}\mathbf{z} - \mathbf{c}) \rangle, \\ &= \underbrace{\bar{f}(\tilde{\mathbf{x}}) + \hat{g}(\tilde{\mathbf{z}}) + \langle \tilde{\boldsymbol{\lambda}}, \tilde{\mathbf{x}} - \tilde{\mathbf{z}} - \tilde{\mathbf{c}} \rangle}_{\stackrel{\text{def}}{=} \tilde{\mathcal{L}}(\tilde{\mathbf{x}}, \tilde{\mathbf{z}}, \tilde{\boldsymbol{\lambda}})}, \end{aligned} \quad (2.71)$$

with a dual-variable substitution $\tilde{\boldsymbol{\lambda}} = \boldsymbol{\lambda} / \rho$. Then, the dual problem is given by

$$\begin{aligned} & \underset{\tilde{\boldsymbol{\lambda}}}{\text{maximize}} \quad \inf_{\tilde{\mathbf{x}}, \tilde{\mathbf{z}}} \mathcal{L}(\tilde{\mathbf{x}}, \tilde{\mathbf{z}}, \tilde{\boldsymbol{\lambda}}), \\ &= \underset{\tilde{\boldsymbol{\lambda}}}{\text{maximize}} \quad \inf_{\tilde{\mathbf{x}}, \tilde{\mathbf{z}}} \tilde{\mathcal{L}}(\tilde{\mathbf{x}}, \tilde{\mathbf{z}}, \tilde{\boldsymbol{\lambda}}), \\ &= \underset{\tilde{\boldsymbol{\lambda}}}{\text{maximize}} \quad - \left(\sup_{\tilde{\mathbf{x}}} \left\{ \langle -\tilde{\boldsymbol{\lambda}}, \tilde{\mathbf{x}} \rangle - \bar{f}(\tilde{\mathbf{x}}) \right\} + \sup_{\tilde{\mathbf{z}}} \left\{ \langle \tilde{\boldsymbol{\lambda}}, \tilde{\mathbf{z}} \rangle - \hat{g}(\tilde{\mathbf{z}}) \right\} + \langle \tilde{\boldsymbol{\lambda}}, \tilde{\mathbf{c}} \rangle \right), \\ &= \underset{\tilde{\boldsymbol{\lambda}}}{\text{maximize}} \quad - \left(\bar{f}^*(-\tilde{\boldsymbol{\lambda}}) + \hat{g}^*(\tilde{\boldsymbol{\lambda}}) + \langle \tilde{\boldsymbol{\lambda}}, \tilde{\mathbf{c}} \rangle \right), \end{aligned} \quad (2.72)$$

which can be rewritten into

$$\underset{\tilde{\lambda}}{\text{minimize}} \quad \tilde{f}^*(-\tilde{\lambda}) + \tilde{g}^*(\tilde{\lambda}) + \langle \tilde{\lambda}, \tilde{c} \rangle = \underset{\tilde{\lambda}}{\text{minimize}} \quad \tilde{f}^*(-\tilde{\lambda}) + \tilde{g}^*(\tilde{\lambda} - \tilde{c}), \quad (2.73)$$

which holds owing to Lemma 2.13. The proof is now concluded. \square

2.8.2 parametrized self-duality

Recall the domain-parametrized Moreau identity from Proposition 2.4, restated here as:

$$\mathbf{v} = \mathbf{Prox}_{f\mathcal{D}^{-1}}(\mathbf{v}) + \mathbf{Prox}_{f^*\mathcal{D}^*}(\mathbf{v}), \quad (2.74)$$

with $\mathbf{v} \in \mathbb{K}$, $f \in \Gamma_0(\mathbb{H})$, where $\mathcal{D} \in \mathfrak{B}(\mathbb{H}, \mathbb{K})$ is injective.

Let $\bar{f}(\mathbf{y}) \stackrel{\text{def}}{=} f \circ (\rho\mathcal{A})^{-1}(\mathbf{y}) - \langle \rho\mathbf{c}, \mathbf{y} \rangle$, $\forall \mathbf{y} \in \mathbb{K}$. Then,

$$\begin{aligned} (\mathcal{I} - \mathbf{Prox}_{\bar{f}})(\mathbf{v}) &= \mathbf{Prox}_{\bar{f}^*}(\mathbf{v}), \\ \iff (\mathcal{I} - \mathbf{Prox}_{\bar{f}})(\mathbf{v}) &= -\mathbf{Prox}_{\bar{f}^*(-\mathcal{I})}(-\mathbf{v}), \\ \iff (2\mathbf{Prox}_{\bar{f}} - \mathcal{I})(\mathbf{v}) &= (2\mathbf{Prox}_{\bar{f}^*(-\mathcal{I})} - \mathcal{I})(-\mathbf{v}). \end{aligned} \quad (2.75)$$

Let $\hat{g}(\mathbf{y}) \stackrel{\text{def}}{=} g \circ (\rho\mathcal{B})^{-1}(\mathbf{y}) + \langle \rho\mathbf{c}, \mathbf{y} \rangle$, $\forall \mathbf{y} \in \mathbb{K}$. Then,

$$\begin{aligned} (\mathcal{I} - \mathbf{Prox}_{\hat{g}})(\mathbf{v}) &= \mathbf{Prox}_{\hat{g}^*}(\mathbf{v}), \\ \iff (\mathcal{I} - 2\mathbf{Prox}_{\hat{g}})(\mathbf{v}) &= (\mathbf{Prox}_{\hat{g}^*} - \mathbf{Prox}_{\hat{g}})(\mathbf{v}), \\ \iff (2\mathbf{Prox}_{\hat{g}} - \mathcal{I})(\mathbf{v}) &= -(\mathbf{Prox}_{\hat{g}^*} - \mathcal{I})(\mathbf{v}). \end{aligned} \quad (2.76)$$

Combining the above two relations, yields

$$\underbrace{(2\mathbf{Prox}_{\bar{f}} - \mathcal{I}) \circ (2\mathbf{Prox}_{\hat{g}} - \mathcal{I})}_{\mathcal{F}_{\text{ADMM}}} = \underbrace{(2\mathbf{Prox}_{\bar{f}^*(-\mathcal{I})} - \mathcal{I}) \circ (2\mathbf{Prox}_{\hat{g}^*} - \mathcal{I})}_{\mathcal{F}_{\text{ADMM}}^*}. \quad (2.77)$$

In view of the primal-dual characterization in Proposition 2.6, we see that the above left-hand-side $\mathcal{F}_{\text{ADMM}}$ corresponds to the primal problem and the right-hand-side $\mathcal{F}_{\text{ADMM}}^*$ to the dual.

Then, the equivalence in (2.77) implies the same primal and dual fixed-point sequences, and hence the same fixed-point, being

$$\zeta^* = \rho\mathcal{A}x^* + \frac{1}{\rho}\lambda^*. \quad (2.78)$$

Moreover, owing to the above $\mathcal{F}_{\text{ADMM}} = \mathcal{F}_{\text{ADMM}}^*$, we have shown (to prove). It follows that the above expression (2.78) is an unscaled fixed-point.

3 Adaptive errors & unified convergence rates

In this section, we consider the convergence rate issue. Below, we first present a general error characterization, which then leads to a worst-case convergence rate. Such a rate is later optimized to find the optimal step-size.

We will use the following definitions:

Definition 3.1. Let $\mathcal{F} : \mathbb{H} \rightarrow \mathbb{H}$, let $L > 0$. Then, \mathcal{F} is

(i) $1/L$ -cocoercive if

$$\frac{1}{L} \|\mathcal{F}\mathbf{x} - \mathcal{F}\mathbf{y}\|^2 \leq \langle \mathcal{F}\mathbf{x} - \mathcal{F}\mathbf{y}, \mathbf{x} - \mathbf{y} \rangle, \quad \forall \mathbf{x}, \mathbf{y} \in \mathbb{H}, \quad (3.1)$$

Moreover, for $L = 1$, \mathcal{F} is called being firmly non-expansive.

(ii) L -Lipschitz continuous if

$$\|\mathcal{F}\mathbf{x} - \mathcal{F}\mathbf{y}\| \leq L \|\mathbf{x} - \mathbf{y}\|, \quad \forall \mathbf{x}, \mathbf{y} \in \mathbb{H} \quad (3.2)$$

Moreover, for $L = 1$, the above \mathcal{F} is called being non-expansive; for $L \in (0, 1)$, it is called a contraction.

Remarks 3.1. By Cauchy-Schwarz inequality, the above (i) implies (ii).

Lemma 3.1. Let $\mathcal{F} : \mathbb{H} \rightarrow \mathbb{H}$ be non-expansive. Then, the averaging $\frac{1}{2}\mathcal{I} + \frac{1}{2}\mathcal{F}$ is firmly non-expansive.

Lemma 3.2. [27, Corollary 23.11] Let $\mathcal{F} : \mathbb{H} \rightarrow \mathbb{H}$ be firmly non-expansive. Then, $\mathcal{I} - \mathcal{F}$ is firmly non-expansive.

3.1 General fixed-point view

3.1.1 Adaptive error characterization

Here, we provide an adaptive error characterization. We obtain two insights: (i) if $L \in (0, 1]$, then the error is guaranteed strictly decreasing at each iteration, until convergence; (ii) even $L \in (1, +\infty)$ (i.e., potentially expansive sequence), it appears still possible that the error remains decreasing (a convergence condition).

Proposition 3.1 (Adaptive error). Suppose $\mathcal{F} : \mathbb{H} \rightarrow \mathbb{H}$ is $1/L$ -cocoercive with $L > 0$. Let process $\zeta^{k+1} = \mathcal{F}\zeta^k$ generate a sequence $\{\zeta^k\}$, with $\zeta^* \in \text{Fix}\mathcal{F}$ denotes the fixed-point (associated with \mathcal{F}), and $k = 0, 1, \dots$ being the iteration number counter.

Then, given an arbitrary initialization ζ^0 , at every k -iteration, the error can be characterized into

$$\underbrace{\|\zeta^{k+1} - \zeta^*\|^2 - \|\zeta^k - \zeta^*\|^2}_{\text{error}} \leq - \underbrace{\left(\|\zeta^{k+1} - \zeta^k\|^2 + \left(\frac{2}{L} - 2 \right) \|\zeta^{k+1} - \zeta^*\|^2 \right)}_{\text{gain}}. \quad (3.3)$$

Moreover, (i) suppose $L \in (0, 1]$. Then, sequence $\{\zeta^k\}$ is guaranteed to converge to a fixed-point (if it exists):

$$\zeta^k \rightarrow \zeta^* \in \text{Fix}\mathcal{F}. \quad (3.4)$$

(ii) suppose $L \in (1, +\infty)$. Then, sequence $\{\zeta^k\}$ is guaranteed to converge to a fixed-point (if it exists), if at every iteration k , the following holds:

$$\|\zeta^{k+1} - \zeta^k\|^2 > \left(2 - \frac{2}{L} \right) \|\zeta^{k+1} - \zeta^*\|^2. \quad (3.5)$$

Proof. First, we show expression (3.3). By definition of $1/L$ -cocoercive, recall (3.1), one has

$$\begin{aligned}
& \|\mathcal{F}\zeta^k - \mathcal{F}\zeta^*\|^2 \leq L\langle \mathcal{F}\zeta^k - \mathcal{F}\zeta^*, \zeta^k - \zeta^* \rangle, \\
\iff & \|\zeta^{k+1} - \zeta^*\|^2 \leq L\langle \zeta^{k+1} - \zeta^*, \zeta^k - \zeta^* \rangle, \\
\iff & 0 \leq L\langle \zeta^{k+1} - \zeta^*, \zeta^k - \zeta^{k+1} \rangle + (L-1)\|\zeta^{k+1} - \zeta^*\|^2, \\
\iff & 0 \leq L\|\zeta^k - \zeta^*\|^2 - L\|\zeta^{k+1} - \zeta^*\|^2 - L\|\zeta^{k+1} - \zeta^k\|^2 + \\
& \quad 2(L-1)\|\zeta^{k+1} - \zeta^*\|^2, \\
\iff & \|\zeta^{k+1} - \zeta^*\|^2 - \|\zeta^k - \zeta^*\|^2 \leq -\|\zeta^{k+1} - \zeta^k\|^2 - \frac{2-2L}{L}\|\zeta^{k+1} - \zeta^*\|^2,
\end{aligned}$$

which gives (3.3).

For case (i), if $L \in (0, 1]$, then the error will be strictly decreasing until convergence. To see this, first, for $L = 1$, we have $2/L - 2 = 0$ and the gain is reduced to a single term $\|\zeta^{k+1} - \zeta^k\|^2$. Clearly, as long as $\zeta^{k+1} \neq \zeta^k$, the gain is non-zero and therefore the error in (3.3) is strictly decreasing. On the other hand, if $\zeta^{k+1} = \zeta^k$, implying convergence, and ζ^{k+1} is a fixed-point of \mathcal{F} , which is (3.4). Now, consider $L \in (0, 1)$. In which case, $2/L - 2 > 0$ and the error decreases strictly faster, and therefore also converges.

For case (ii), essentially, as long as the right-hand-side of (3.3) is strictly negative for all iterations (until convergence), then the error on its left-hand-side must converge to 0, which corresponds to our last claim in (3.5).

The proof is now concluded. \square

Remarks 3.2 (simplicity & abstraction). Above, we provide a simple error characterization. The simplicity owes to the abstraction, that we avoid discussing the specific structure of the fixed-point operator. A typical structure is the sum of two monotone operators, see Moursi and Vandenberghe [31] for a comprehensive investigation and Giselsson and Boyd [8] for a different characterization and applications.

3.1.2 Intrinsic almost-linear rate

Here, we provide two types of rates. Particularly, we show that — the sub-linear rate $O(1/(k+1))$ is intrinsically almost linear, in the sense that it will instantly become linear with an arbitrarily small improvement on the constant L .

Proposition 3.2 (Worst-case rates). *For the above defined sequence $\{\zeta^k\}$:*

(i) Suppose $L = 1$, then

$$\|\zeta^{k+1} - \zeta^k\|^2 \leq \frac{1}{k+1}\|\zeta^* - \zeta^0\|^2. \quad (\text{sub-linear; intrinsic})$$

(ii) Suppose $L \in (0, 1)$. Let $\delta = \frac{2}{L} - 1$. Then,

$$\begin{aligned}
\|\zeta^{k+1} - \zeta^k\|^2 & \leq \frac{\delta - 1}{\delta^{(k+1)} - 1}\|\zeta^* - \zeta^0\|^2, \\
& \leq \delta^{-k}\|\zeta^* - \zeta^0\|^2. \quad (\text{linear; strong assumption})
\end{aligned}$$

Proof. The proof for the above two cases are similar.

• To start, we prove (**linear; strong assumption**), which is slightly more general. In view of Proposition 3.1, rearrange (3.3) into

$$\|\zeta^{t+1} - \zeta^t\|^2 \leq \|\zeta^t - \zeta^\star\|^2 - \delta \|\zeta^{t+1} - \zeta^\star\|^2. \quad (3.6)$$

Sum over all t iterations till the k -th one:

$$\sum_{t=0}^k \delta^t \|\zeta^{t+1} - \zeta^t\|^2 \leq \|\zeta^\star - \zeta^0\|^2. \quad (\text{result 1})$$

Since $1/L$ -cocoercive is always L -Lipschitz continuous, see Remark 3.1. Then, following from (3.2), we arrive at

$$\|\zeta^{t+1} - \zeta^t\| \leq \|\zeta^t - \zeta^{t-1}\| \leq \|\zeta^{t-2} - \zeta^{t-3}\| \leq \dots \quad (3.7)$$

Moreover, since $\delta > 0$, we can add it to both sides of the inequality. That is, for any $t \leq k$, we have

$$\delta^t \|\zeta^{k+1} - \zeta^k\| \leq \delta^t \|\zeta^{t+1} - \zeta^t\|. \quad (3.8)$$

Sum over $t = 0, 1, \dots, k$, yielding

$$\begin{aligned} \sum_{t=0}^k \delta^t \|\zeta^{k+1} - \zeta^k\|^2 &\leq \sum_{t=0}^k \delta^t \|\zeta^{t+1} - \zeta^t\|^2, \\ \Leftrightarrow \frac{1 - \delta^{(k+1)}}{1 - \delta} \|\zeta^{k+1} - \zeta^k\|^2 &\leq \sum_{t=0}^k \delta^t \|\zeta^{t+1} - \zeta^t\|^2, \end{aligned} \quad (\text{result 2}) \quad (3.9)$$

Adding (result 1) and (result 2) yields the convergence rate bound

$$\|\zeta^{k+1} - \zeta^k\|^2 \leq \frac{\delta - 1}{\delta^{(k+1)} - 1} \|\zeta^\star - \zeta^0\|^2. \quad (3.10)$$

Furthermore, since $\delta = \frac{2}{L} - 1 > 1$, we have

$$\frac{\delta - 1}{\delta^{(k+1)} - 1} \leq \frac{\delta}{\delta^{(k+1)}} = \delta^{-k}, \quad (3.11)$$

which gives (**linear; strong assumption**).

• Now, we prove (**sub-linear; intrinsic**), which shares similar arguments with $\delta = 1$. To avoid repeating, we directly start from (result 1) and (3.9), which now become

$$\sum_{t=0}^k \|\zeta^{t+1} - \zeta^t\|^2 \leq \|\zeta^\star - \zeta^0\|^2, \quad (3.12)$$

$$\sum_{t=0}^k \|\zeta^{k+1} - \zeta^k\|^2 \leq \sum_{t=0}^k \|\zeta^{t+1} - \zeta^t\|^2. \quad (3.13)$$

Adding the above two yields

$$\|\zeta^{k+1} - \zeta^k\|^2 \leq \frac{1}{k+1} \|\zeta^\star - \zeta^0\|^2, \quad (3.14)$$

which concludes the proof. \square

Remarks 3.3 (literature connections & novelty). The sub-linear result itself as in (sub-linear; intrinsic) is well-known in the literature, see typical work from Ryu and Yin [9, Theorem 1, sec. 2.4.2] and earlier establishment through variational inequality by Bingsheng and Xiaoming [32]. For the linear rate, it can be achieved by various different strong assumptions, see e.g. [8, 31].

Our novelty lies on at least the following two aspects: (i) a new and simple proof, which reveals an almost-linear nature for the basic case; (ii) For the Lipschitz case, rather than a linear rate δ^{-k} , the direct consequence of our proof is a stronger one $(\delta - 1)/(\delta^{(k+1)} - 1)$, and appears admitting potential to be further tightened. Calculating a stronger factor could be beneficial, including important theoretical insights and potentially a new approach to further improve the convergence rate.

3.2 Primal-dual sequences: reciprocal rates

In the previous section, we characterize the general convergence behaviour of a fixed-point sequence. Recall that the ADMM fixed-point is a combination of the primal and dual parts, i.e., $\zeta^{k+1} = \rho \mathcal{A}x^{k+1} + \lambda^k/\rho$, see (2.64). Here, we investigate the convergence behaviour of the primal and dual parts separately.

Proposition 3.3. *Consider the ADMM (scaled form) or (prox. ADMM). Given arbitrary non-zero step-size $\rho \neq 0$ and arbitrary initialization ζ^0 . Then,*

$$\begin{aligned} \|\mathcal{A}x^{k+2} - \mathcal{A}x^{k+1}\|^2 &\leq \frac{1}{k+1} \cdot \|\zeta^* - \zeta^0\|^2 \cdot \frac{1}{\rho^2}, \\ &= \frac{1}{k+1} \cdot \|\mathcal{A}x^* + \frac{1}{\rho^2}\lambda^* - \frac{1}{\rho}\zeta^0\|^2, \end{aligned} \quad (\text{primal})$$

and

$$\begin{aligned} \|\lambda^{k+1} - \lambda^k\|^2 &\leq \frac{1}{k+1} \cdot \|\zeta^* - \zeta^0\|^2 \cdot \rho^2, \\ &= \frac{1}{k+1} \cdot \|\rho^2 \mathcal{A}x^* + \lambda^* - \rho\zeta^0\|^2. \end{aligned} \quad (\text{dual})$$

Proof. The proof follows directly from Proposition 2.5. We will employ the same scaled variables and functions there, restated here as

$$\tilde{x}^k \stackrel{\text{def}}{=} \rho \mathcal{A}x^k, \quad \tilde{z}^k \stackrel{\text{def}}{=} \rho \mathcal{B}z^k, \quad \tilde{\lambda}^k \stackrel{\text{def}}{=} \frac{1}{\rho} \lambda^k, \quad \tilde{c} \stackrel{\text{def}}{=} \rho c, \quad (3.15)$$

and

$$\bar{f}(\mathbf{y}) \stackrel{\text{def}}{=} f \circ (\rho \mathcal{A})^{-1}(\mathbf{y}) - \langle \rho c, \mathbf{y} \rangle, \quad (3.16)$$

$$\hat{g}(\mathbf{y}) \stackrel{\text{def}}{=} g \circ (\rho \mathcal{B})^{-1}(\mathbf{y}) + \langle \rho c, \mathbf{y} \rangle, \quad \forall \mathbf{y} \in \mathbb{K}. \quad (3.17)$$

First, for the scaled primal iterate, we have

$$\tilde{x}^{k+1} = \text{Prox}_{f(\rho \mathcal{A})^{-1}}(2\tilde{c} + 2\tilde{z}^k - \zeta^k), \quad (3.18)$$

$$= \text{Prox}_{f(\rho \mathcal{A})^{-1}} \circ \left(\tilde{c} + (2\text{Prox}_{g(\rho \mathcal{B})^{-1}} - \mathcal{I})(\zeta^k - \tilde{c}) \right), \quad (3.19)$$

$$= \underbrace{\text{Prox}_{\bar{f}} \circ (2\text{Prox}_{\hat{g}} - \mathcal{I})}_{\stackrel{\text{def}}{=} \mathcal{F}_x} \zeta^k, \quad (3.20)$$

The last line is a composition of a firmly non-expansive operator and a non-expansive operator, which is at least non-expansive. Hence,

$$\|\tilde{\mathbf{x}}^{k+2} - \tilde{\mathbf{x}}^{k+1}\|^2 = \|\mathcal{F}_x \zeta^{k+1} - \mathcal{F}_x \zeta^k\|^2 \leq \|\zeta^{k+1} - \zeta^k\|^2 \leq \frac{1}{k+1} \|\zeta^\star - \zeta^0\|^2. \quad (3.21)$$

Invoke definition (3.15), then

$$\|\rho \mathcal{A} \mathbf{x}^{k+2} - \rho \mathcal{A} \mathbf{x}^{k+1}\|^2 \leq \frac{1}{k+1} \|\zeta^\star - \zeta^0\|^2 = \frac{1}{k+1} \|\rho \mathcal{A} \mathbf{x}^\star + \boldsymbol{\lambda}^\star / \rho - \zeta^0\|^2. \quad (3.22)$$

Since $\rho \neq 0$, we can divide both sides above with ρ^2 , which gives (primal).

Similarly, for the dual iterates, we have

$$\begin{aligned} \tilde{\boldsymbol{\lambda}}^k &= \zeta^k - \tilde{\mathbf{z}}^k - \tilde{\mathbf{c}} = (\zeta^k - \tilde{\mathbf{c}}) - \mathbf{Prox}_{g(\rho\mathcal{B})^{-1}}(\zeta^k - \tilde{\mathbf{c}}), \\ &= \underbrace{\left(\mathcal{I} - \mathbf{Prox}_{\hat{g}} \right)}_{\stackrel{\text{def}}{=} \mathcal{F}_\lambda} \zeta^k, \end{aligned} \quad (3.23)$$

where \mathcal{F}_λ is firmly non-expansive (recall Lemma 3.2), which implies non-expansiveness. Following the same arguments as above, we have

$$\|\tilde{\boldsymbol{\lambda}}^{k+1} - \tilde{\boldsymbol{\lambda}}^k\|^2 \leq \|\mathcal{F}_\lambda \zeta^{k+1} - \mathcal{F}_\lambda \zeta^k\|^2 \leq \|\zeta^{k+1} - \zeta^k\|^2 \leq \frac{1}{k+1} \|\zeta^\star - \zeta^0\|^2, \quad (3.24)$$

where $\tilde{\boldsymbol{\lambda}}^k \stackrel{\text{def}}{=} \boldsymbol{\lambda}^k / \rho$. Since $\rho \neq 0$, we can scale the above relations with ρ^2 , which gives (dual). The proof is now concluded. \square

Remarks 3.4 (Reciprocal residue behaviours). In Boyd et. al. [1, sec. 3.4.1], the authors point out that: ‘The ADMM update equations suggest that large values of step-sizes place a large penalty on violations of primal feasibility and so tend to produce small primal residuals. Conversely, ...’

Their interpretation via residues do coincide with our results. In fact, under our measures, the primal and dual admit exactly reciprocal behaviours:

$$\|\mathcal{A} \mathbf{x}^{k+2} - \mathcal{A} \mathbf{x}^{k+1}\|^2 \leq \frac{1}{k+1} \cdot \frac{1}{\rho^2} \cdot \|\zeta^\star - \zeta^0\|^2, \quad (3.25)$$

$$\|\boldsymbol{\lambda}^{k+1} - \boldsymbol{\lambda}^k\|^2 \leq \frac{1}{k+1} \cdot \rho^2 \cdot \|\zeta^\star - \zeta^0\|^2. \quad (3.26)$$

From above we see that a larger choice of step-size ρ tends to speed-up the primal iterates convergence, since the right-hand-side contains an additional factor $1/\rho^2$. Similar arguments hold for the dual.

Meanwhile, we emphasize that this observation is only a general trend, i.e., a larger step-size does not guarantee to improve the primal convergence, since there is another factor $\zeta^\star = \rho \mathcal{A} \mathbf{x}^\star + \boldsymbol{\lambda}^\star / \rho$, which also changes with step-size ρ .

4 Optimal step-size selection

In this section, we determine an optimal step-size choice by minimizing the worst-case convergence rates established in the previous section.

Let us note that the step-size selection scheme should be as simple as possible, since otherwise there exists risk that the overall efficiency decreases (calculating step-size choice adds a cost). Ideally, we prefer a closed-form choice, which will be guaranteed by our proposed method.

4.1 Towards a simple general principle

We consider minimizing the worst-case convergence rates in Proposition 3.2, restated here as

$$\|\zeta^{k+1} - \zeta^k\|^2 \leq \frac{1}{k+1} \|\zeta^* - \zeta^0\|^2, \quad L = 1, \quad (4.1)$$

$$\|\zeta^{k+1} - \zeta^k\|^2 \leq \frac{\delta - 1}{\delta^{(k+1)} - 1} \|\zeta^* - \zeta^0\|^2, \quad \delta = \frac{2}{L} - 1, \quad L \in (0, 1). \quad (4.2)$$

Substituting the ADMM-type fixed-point expression, we obtain the following two step-size selection schemes:

$$\underset{\rho \neq 0}{\text{minimize}} \quad \|\rho \mathcal{A}x^* + \lambda^*/\rho - \zeta^0\|^2, \quad (\text{basic})$$

$$\underset{\rho \neq 0}{\text{minimize}} \quad \frac{\delta - 1}{\delta^{(k+1)} - 1} \|\rho \mathcal{A}x^* + \lambda^*/\rho - \zeta^0\|^2, \quad (\text{Lipschitz})$$

where term $1/(k+1)$ is omitted in (basic) (iteration number counter k is clearly independent here). To determine which formulation to employ, let us note that:

- (basic) is generally applicable to all ADMM-type convex programs, since $\mathcal{F}_{\text{ADMM}}$ is intrinsically firmly non-expansive ($L = 1$), without need of any additional assumptions.
- (Lipschitz) requires calculating factor $\delta = \frac{2}{L} - 1$, i.e., the cocoercive constant $L < 1$, which is not guaranteed in general, and therefore this formulation is a tailored method. Also, this approach is complicated, due to L is related to the step-size ρ , see e.g. [8, 31] for the specific relation in the sum of two monotone operators problem setting. Moreover, if the step-size is changing (needed for practical use, see later Sec. 4.5), we then need adaptively calculating L , which adds additional cost compared to (basic). Therefore, if $L \approx 1$, this formulation is not necessary better (despite some structure exploited). Of course, if $L \ll 1$, implying highly structured data, we do expect efficiency advantages.

Overall, since we aim to establish a simple and general selection scheme in this work, we employ (basic). We leave formulation (Lipschitz) to the future work in the context of some highly-structured applications.

4.1.1 Conventional failure

Before solving (basic) which employs our unscaled fixed-point, we first show that the conventional fixed-point expressions will fail. In the literature, there exist two fixed-point expressions for ADMM:

$$\underbrace{\zeta_1^* = \mathcal{A}x^* + \lambda^*/\gamma}_{\text{obtained via primal}}, \quad \underbrace{\zeta_2^* = \gamma \mathcal{A}x^* + \lambda^*}_{\text{obtained via dual}}. \quad (4.3)$$

see ζ_1^* from [9, sec. 3.1], corresponding to the primal problem, and ζ_2^* from [9, sec. 3.2] (see also [22]), corresponding to the dual problem.

Consider ζ_1^* first, for comparison purpose, we denote its step-size as γ_1 . Substitute it to bound (4.1):

$$\underset{\gamma_1 > 0}{\text{minimize}} \quad \|\mathcal{A}\mathbf{x}^* + \boldsymbol{\lambda}^*/\gamma_1 - \zeta^0\|^2, \quad (4.4)$$

$$= \underset{\gamma_1 > 0}{\text{minimize}} \quad \frac{1}{\gamma_1^2} \|\boldsymbol{\lambda}^*\|^2 + \frac{2}{\gamma_1} \langle \mathcal{A}\mathbf{x}^* - \zeta^0, \boldsymbol{\lambda}^* \rangle + \|\mathcal{A}\mathbf{x}^* - \zeta^0\|^2. \quad (4.5)$$

with solution

$$\gamma_1^* = \begin{cases} -\frac{\|\boldsymbol{\lambda}^*\|^2}{\langle \mathcal{A}\mathbf{x}^* - \zeta^0, \boldsymbol{\lambda}^* \rangle} & \langle \mathcal{A}\mathbf{x}^* - \zeta^0, \boldsymbol{\lambda}^* \rangle < 0, \\ \downarrow 0 & \langle \mathcal{A}\mathbf{x}^* - \zeta^0, \boldsymbol{\lambda}^* \rangle > 0, \\ +\infty & \langle \mathcal{A}\mathbf{x}^* - \zeta^0, \boldsymbol{\lambda}^* \rangle = 0, \end{cases} \quad (\text{primal case})$$

where $\downarrow 0$ denotes approaching 0 from the positive orthant.

Consider ζ_2^* . Similarly, denote its corresponding step-size as γ_2 , we obtain

$$\underset{\gamma_2 > 0}{\text{minimize}} \quad \|\gamma_2 \mathcal{A}\mathbf{x}^* + \boldsymbol{\lambda}^* - \zeta^0\|^2, \quad (4.6)$$

$$= \underset{\gamma_2 > 0}{\text{minimize}} \quad \|\boldsymbol{\lambda}^* - \zeta^0\|^2 + 2\gamma_2 \langle \mathcal{A}\mathbf{x}^*, \boldsymbol{\lambda}^* - \zeta^0 \rangle + \gamma_2^2 \|\mathcal{A}\mathbf{x}^*\|^2. \quad (4.7)$$

with solution

$$\gamma_2^* = \begin{cases} -\frac{\langle \mathcal{A}\mathbf{x}^*, \boldsymbol{\lambda}^* - \zeta^0 \rangle}{\|\mathcal{A}\mathbf{x}^*\|^2} & \langle \mathcal{A}\mathbf{x}^*, \boldsymbol{\lambda}^* - \zeta^0 \rangle < 0, \\ +\infty & \langle \mathcal{A}\mathbf{x}^*, \boldsymbol{\lambda}^* - \zeta^0 \rangle > 0, \\ \downarrow 0 & \langle \mathcal{A}\mathbf{x}^*, \boldsymbol{\lambda}^* - \zeta^0 \rangle = 0. \end{cases} \quad (\text{dual case})$$

We see that γ_1^* and γ_2^* suggest different choices. However, in (4.3) the step-size is the same, i.e., $\gamma_1 = \gamma_2$, see derivation details from [9, sec. 3.1, 3.2].

Additionally, for practical evidence, consider the standard semidefinite programming. The solution there is often given as a matrix primal-dual pair $(\mathbf{X}^*, \boldsymbol{\Lambda}^*)$, satisfying $\langle \mathbf{X}^*, \boldsymbol{\Lambda}^* \rangle = 0$ (where $\mathcal{A} = \mathcal{I}$ vanishes). Then, under zero initialization $\zeta^0 = \mathbf{0}$, the above results indicate that the step-size should always be chosen $+\infty$ for the primal problem and $\downarrow 0$ for the dual. Such extreme choices are clearly against practical experiences.

Overall, the above (primal case) and (dual case) should not be the correct answers. Their problematic behaviours could be why the optimal step-size issue is considered open in the literature, as pointed out in [6, Sec. 1.2, First-order methods], [9, Sec. 8, Parameter selection].

4.2 General optimal step-size (fixed-point view)

Here, we solve (basic). For better connection to the current literature, we emphasize that the relation between our domain step-size $\rho \neq 0$ and the classical range step-size $\gamma > 0$ is, recall Lemma 2.1:

$$\underset{\text{classical range step-size}}{\gamma} = \underset{\text{domain step-size}}{\rho^2}. \quad (4.8)$$

Now, invoke (basic), we arrive at:

$$\underset{\rho \neq 0}{\text{minimize}} \quad \|\rho \mathcal{A}\mathbf{x}^* + \boldsymbol{\lambda}^*/\rho - \zeta^0\|^2, \quad (\text{opt. sel.})$$

where $\zeta^0 = \rho_0 \mathcal{A}x^0 + \lambda^0 / \rho_0$ denotes an arbitrary fixed-point initialization, with x^0 , λ^0 and $\rho_0 \neq 0$ denote the primal, dual, and step-size initializations, respectively.

Expand all ρ -related terms:

$$\underset{\rho \neq 0}{\text{minimize}} \quad \rho^2 \|\mathcal{A}x^*\|^2 + \frac{1}{\rho^2} \|\lambda^*\|^2 - 2\rho \langle \mathcal{A}x^*, \zeta^0 \rangle - \frac{2}{\rho} \langle \lambda^*, \zeta^0 \rangle. \quad (4.9)$$

The first-order optimality condition yields

$$2\rho \|\mathcal{A}x^*\|^2 - \frac{2}{\rho^3} \|\lambda^*\|^2 - 2\langle \mathcal{A}x^*, \zeta^0 \rangle + \frac{2}{\rho^2} \langle \lambda^*, \zeta^0 \rangle = 0. \quad (4.10)$$

Since $\rho \neq 0$, the above is equivalent to solving the following polynomial:

$$\rho^4 \|\mathcal{A}x^*\|^2 - \rho^3 \langle \mathcal{A}x^*, \zeta^0 \rangle + \rho \langle \lambda^*, \zeta^0 \rangle - \|\lambda^*\|^2 = 0, \quad \rho \neq 0, \quad (4.11)$$

which is at most degree-4, and therefore always admits a closed-form solution, specified below.

4.2.1 closed-form expressions

For the sake of convenience, we adopt the following norm measures:

$$\|\mathcal{A}x^*\| = 0 \iff x^* = \mathbf{0}, \quad (4.12)$$

$$\|\lambda^*\| = 0 \iff \lambda^* = \mathbf{0}, \quad (4.13)$$

where \mathcal{A} is injective. Now, we specify the closed-form solution:

- **(Trivial.)** Suppose $\|\mathcal{A}x^*\| = 0, \|\lambda^*\| = 0$. Then, all feasible choices are equivalent, i.e., $\rho^* \in [-\infty, +\infty] \setminus \{0\}$ (since the objective in (opt. sel.) is a constant).

- **(Partly trivial – useful primal.)** Suppose $\|\mathcal{A}x^*\| \neq 0, \|\lambda^*\| = 0$. (i) For zero initialization $\zeta^0 = \mathbf{0}$, the optimal choice $\rho^* \rightarrow 0$, i.e., infinitely close to zero (absolute-value sense); (ii) For non-zero initialization $\zeta^0 \neq \mathbf{0}$, then $\rho^* = \langle \mathcal{A}x^*, \zeta^0 \rangle / \|\mathcal{A}x^*\|^2$.

- **(Partly trivial – useful dual.)** Suppose $\|\mathcal{A}x^*\| = 0, \|\lambda^*\| \neq 0$. Similar to above: (i) Set $\zeta^0 = \mathbf{0}$, then $\rho^* \rightarrow \infty$, i.e., infinitely close to infinity (absolute-value sense); (ii) Set $\zeta^0 \neq \mathbf{0}$, then $\rho^* = \|\lambda^*\|^2 / \langle \lambda^*, \zeta^0 \rangle$.

- **(Non-trivial.)** Suppose $\|\mathcal{A}x^*\| \neq 0, \|\lambda^*\| \neq 0$. (i) Set $\zeta^0 = \mathbf{0}$, then $\rho^* = \pm \sqrt{\|\lambda^*\| / \|\mathcal{A}x^*\|}$; (ii) Set $\zeta^0 \neq \mathbf{0}$, then the solution is specified below.

For light of notations, we rewrite the polynomial in (4.11) as

$$a\rho^4 + b\rho^3 + d\rho + e = 0. \quad (4.14)$$

which, in our case, admits the following four roots:

$$\rho = \begin{cases} \frac{1}{2}(-\frac{b}{2a} - u_4 - \sqrt{u_5 - u_6}), \\ \frac{1}{2}(-\frac{b}{2a} - u_4 + \sqrt{u_5 - u_6}), \\ \frac{1}{2}(-\frac{b}{2a} + u_4 - \sqrt{u_5 + u_6}), \\ \frac{1}{2}(-\frac{b}{2a} + u_4 + \sqrt{u_5 + u_6}), \end{cases} \quad (4.15)$$

where

$$u_4 = \sqrt{\frac{b^2}{4a^2} + u_3}, \quad u_5 = \frac{b^2}{2a^2} - u_3, \quad u_6 = -\frac{\frac{b^3}{a^3} + \frac{8d}{a}}{4u_4},$$

and where

$$u_1 = \frac{\sqrt{27}}{2}(ad^2 + b^2e), u_2 = u_1 + \sqrt{(bd - 4ae)^3 + u_1^2}, u_3 = \frac{1}{\sqrt{3a}}(\sqrt[3]{u_2} - \frac{bd - 4ae}{\sqrt[3]{u_2}}).$$

At this stage, we do not realize a direct way to distinguish the above 4 roots. We would suggest: first remove complex roots (since we consider a real Hilbert space; typically, two real roots and two complex roots), then find the best one via

$$\rho^* = \underset{\rho \in (4.15)}{\operatorname{argmin}} \|\rho \mathcal{A}x^* + \lambda^*/\rho - \zeta^0\|^2, \quad (4.16)$$

which adds negligible cost owing to the closed-form expressions.

Remarks 4.1 (complex variables). For some applications, the primal-dual solutions may be complex. In which case, one may simply solve:

$$\rho^4 \|\mathcal{A}x^*\|^2 - \rho^3 \langle \mathcal{A}x^*, \zeta^0 \rangle_{\mathbb{R}} + \rho \langle \lambda^*, \zeta^0 \rangle_{\mathbb{R}} - \|\lambda^*\|^2 = 0, \quad (4.17)$$

where $\langle \cdot, \cdot \rangle_{\mathbb{R}}$ denotes the real part of an inner product.

4.3 Optimal rates

4.3.1 general (zero initialization): balanced rates

Below we will see that, under zero initialization, employ the optimal step-size. Then, the worst-case convergence rates of the normalized primal, dual and fixed-point sequences are the same.

Proposition 4.1. *Suppose $\|\mathcal{A}x^*\| \neq 0$, $\|\lambda^*\| \neq 0$. Set $\zeta^0 = \mathbf{0}$ and choose step-size $\rho^* = \pm \sqrt{\|\lambda^*\|/\|\mathcal{A}x^*\|}$. Let*

$$\theta = \arccos \frac{\langle \mathcal{A}x^*, \lambda^* \rangle}{\|\mathcal{A}x^*\| \|\lambda^*\|}. \quad (\text{intrinsic angle})$$

Then,

$$\frac{\|\mathcal{A}x^{k+2} - \mathcal{A}x^{k+1}\|^2}{\|\mathcal{A}x^*\|^2} \leq \frac{2}{k+1} (1 + \cos \theta), \quad (\text{primal})$$

$$\frac{\|\lambda^{k+1} - \lambda^k\|^2}{\|\lambda^*\|^2} \leq \frac{2}{k+1} (1 + \cos \theta), \quad (\text{dual})$$

$$\frac{\|\zeta^{k+1} - \zeta^k\|^2}{\|\mathcal{A}x^*\| \|\lambda^*\|} \leq \frac{2}{k+1} (1 + \cos \theta). \quad (\text{fixed-point})$$

Proof. Following from Proposition 3.3, given $\zeta^0 = \mathbf{0}$ and the optimal step-size ρ^* , we arrive at

$$\|\mathcal{A}x^{k+2} - \mathcal{A}x^{k+1}\|^2 \leq \frac{1}{k+1} \left\| \mathcal{A}x^* + \frac{1}{(\rho^*)^2} \lambda^* - \mathbf{0} \right\|^2. \quad (4.18)$$

$$\|\lambda^{k+1} - \lambda^k\|^2 \leq \frac{1}{k+1} \|(\rho^*)^2 \mathcal{A}x^* + \lambda^* - \mathbf{0}\|^2, \quad (4.19)$$

$$\|\zeta^{k+1} - \zeta^k\|^2 \leq \frac{1}{k+1} \|\rho^* \mathcal{A}x^* + \lambda^*/\rho^* - \mathbf{0}\|^2. \quad (4.20)$$

Invoke $\rho^* = \pm\sqrt{\|\boldsymbol{\lambda}^*\|/\|\mathcal{A}\mathbf{x}^*\|}$ and θ defined in (intrinsic angle), and rearrange the terms concludes the proof. \square

Remarks 4.2 (intrinsic efficiency). Given a certain convex program, let us note that its optimal solution is fixed, hence θ is fixed. Then, from above, we see that the efficiency of different convex programs (under zero initialization) can be characterized by $\cos \theta \in [-1, 1]$.

Remarks 4.3 (Successor to the literature adaptive principle?). As pointed out in Boyd et. al. [1, sec. 3.4.1], a simple adaptive step-size selection scheme that often works well is (e.g. [33, 34]):

$$\gamma^{k+1} = \begin{cases} \tau^{\text{incr}} \gamma^k & \text{if } \|\mathbf{r}^k\| > \mu \|\mathbf{s}^k\|, \\ \gamma^k / \tau^{\text{decr}} & \text{if } \|\mathbf{r}^k\| < \mu \|\mathbf{s}^k\|, \\ \gamma^k & \text{otherwise,} \end{cases} \quad (4.21)$$

where \mathbf{r}^k and \mathbf{s}^k are primal and dual residues, respectively. Typical choices might be $\mu = 10$, $\tau^{\text{incr}} = \tau^{\text{decr}} = 2$. ‘The idea behind this penalty parameter update is to try to keep the primal and dual residual norms within a factor of μ of one another as they both converge to zero.’ [1]

Such an idea appears consistent here — the optimal step-size is the one that makes the (normalized) primal and dual iterates converge in the same speed. Compared to the above heuristic adaptive scheme, our step-size choice controls the primal and dual sequence to be the same speed, rather than theirs within factor μ (typically $\mu = 10$). In this sense, ours seems a better choice.

Remarks 4.4 (single stopping threshold). Owing to the balanced rates, we may simplify the stopping criteria for ADMM into a single error threshold (under zero initialization). This is a simplification to the multiple thresholds in the current literature, see [1].

4.3.2 partly trivial (zero initialization): fixed non-trivial rate

Below, we show that if either the primal or dual solution is a zero vector (trivial), then the convergence rate of the non-trivial iterate is independent of the step-size selection.

Proposition 4.2. (i) Suppose $\|\mathcal{A}\mathbf{x}^*\| \neq 0$, $\|\boldsymbol{\lambda}^*\| = 0$. Set $\boldsymbol{\zeta}^0 = \mathbf{0}$. Then,

$$\|\mathcal{A}\mathbf{x}^{k+2} - \mathcal{A}\mathbf{x}^{k+1}\|^2 \leq \frac{1}{k+1} \cdot \|\mathcal{A}\mathbf{x}^*\|^2, \quad (\text{primal})$$

$$\|\boldsymbol{\lambda}^{k+1} - \boldsymbol{\lambda}^k\|^2 \leq \frac{1}{k+1} \cdot \|\mathcal{A}\mathbf{x}^*\|^2 \cdot \rho^4, \quad (\text{trivial dual})$$

$$\|\boldsymbol{\zeta}^{k+1} - \boldsymbol{\zeta}^k\|^2 \leq \frac{1}{k+1} \cdot \|\mathcal{A}\mathbf{x}^*\|^2 \cdot \rho^2. \quad (\text{fixed-point})$$

(ii) Suppose $\|\mathcal{A}\mathbf{x}^*\| = 0$, $\|\boldsymbol{\lambda}^*\| \neq 0$. Set $\boldsymbol{\zeta}^0 = \mathbf{0}$. Then,

$$\|\boldsymbol{\lambda}^{k+1} - \boldsymbol{\lambda}^k\|^2 \leq \frac{1}{k+1} \cdot \|\boldsymbol{\lambda}^*\|^2, \quad (\text{dual})$$

$$\|\mathcal{A}\mathbf{x}^{k+2} - \mathcal{A}\mathbf{x}^{k+1}\|^2 \leq \frac{1}{k+1} \cdot \|\boldsymbol{\lambda}^*\|^2 \cdot \frac{1}{\rho^4}, \quad (\text{trivial primal})$$

$$\|\boldsymbol{\zeta}^{k+1} - \boldsymbol{\zeta}^k\|^2 \leq \frac{1}{k+1} \cdot \|\boldsymbol{\lambda}^*\|^2 \cdot \frac{1}{\rho^2}. \quad (\text{fixed-point})$$

Proof. The proof follows straightforwardly from Proposition 3.3. \square

Remarks 4.5 (independence & optimality interpretation). Interestingly, under zero initialization, the above result implies that the step-size selection is independent of the non-trivial sequence worst-case rate. This will be verified numerically in Sec. 5.2, which shows a complete independence in practice.

Moreover, we see that the previously derived step-size choice is optimal, in the sense that the trivial sequence convergence rate is most accelerated. Specifically, for the above case (i), recall the optimal step-size being $\rho^* \rightarrow 0$. Substituting it to the above, only the dual and fixed-point sequence one is affected, with their upper bounds being:

$$\lim_{\rho^* \rightarrow 0} (\rho^*)^4 \cdot \frac{\|\mathcal{A}\mathbf{x}^*\|^2}{k+1} = 0, \quad \lim_{\rho^* \rightarrow 0} (\rho^*)^2 \cdot \frac{\|\mathcal{A}\mathbf{x}^*\|^2}{k+1} = 0. \quad (4.22)$$

Similar arguments hold for case (ii).

4.3.3 partly trivial (non-zero initialization): initialization angle

Here, we consider an arbitrary non-zero initialization, where the convergence rate of the non-trivial sequence is now related to the step-size choices and can be improved compared to the previous fixed one in Proposition 4.2. The maximum improvement depends on the initialization angle only.

Proposition 4.3 (balanced/fixed-point view). *(i) Suppose $\|\mathcal{A}\mathbf{x}^*\| \neq 0$, $\|\boldsymbol{\lambda}^*\| = 0$. Set any initialization $\boldsymbol{\zeta}^0 \neq \mathbf{0}$. Let*

$$\omega_1 = \arccos \frac{\langle \mathcal{A}\mathbf{x}^*, \boldsymbol{\zeta}^0 \rangle}{\|\mathcal{A}\mathbf{x}^*\| \|\boldsymbol{\zeta}^0\|}. \quad (\text{initial primal angle})$$

Choose step-size to be $\rho^ = \frac{\|\boldsymbol{\zeta}^0\|}{\|\mathcal{A}\mathbf{x}^*\|} \cos \omega_1$. Then,*

$$\|\mathcal{A}\mathbf{x}^{k+2} - \mathcal{A}\mathbf{x}^{k+1}\|^2 \leq \frac{1}{k+1} \cdot \|\mathcal{A}\mathbf{x}^*\|^2 \cdot \tan^2 \omega_1, \quad (\text{non-trivial})$$

$$\|\boldsymbol{\lambda}^{k+1} - \boldsymbol{\lambda}^k\|^2 \leq \frac{1}{k+1} \cdot \frac{\|\boldsymbol{\zeta}^0\|^4}{4\|\mathcal{A}\mathbf{x}^*\|^2} \cdot \sin^2 2\omega_1. \quad (\text{trivial dual})$$

$$\|\boldsymbol{\zeta}^{k+1} - \boldsymbol{\zeta}^k\|^2 \leq \frac{1}{k+1} \cdot \|\boldsymbol{\zeta}^0\|^2 \cdot \sin^2 \omega_1. \quad (\text{fixed-point})$$

(ii) Suppose $\|\mathcal{A}\mathbf{x}^\| = 0$, $\|\boldsymbol{\lambda}^*\| \neq 0$. Set any initialization $\boldsymbol{\zeta}^0 \neq \mathbf{0}$. Let*

$$\omega_2 = \arccos \frac{\langle \boldsymbol{\lambda}^*, \boldsymbol{\zeta}^0 \rangle}{\|\boldsymbol{\lambda}^*\| \|\boldsymbol{\zeta}^0\|}. \quad (\text{initial dual angle})$$

Choose step-size to be $\rho^ = 1/(\frac{\|\boldsymbol{\zeta}^0\|}{\|\boldsymbol{\lambda}^*\|} \cos \omega_2)$. Then,*

$$\|\boldsymbol{\lambda}^{k+1} - \boldsymbol{\lambda}^k\|^2 \leq \frac{1}{k+1} \cdot \|\boldsymbol{\lambda}^*\|^2 \cdot \tan^2 \omega_2, \quad (\text{non-trivial})$$

$$\|\mathcal{A}\mathbf{x}^{k+2} - \mathcal{A}\mathbf{x}^{k+1}\|^2 \leq \frac{1}{k+1} \cdot \frac{\|\boldsymbol{\zeta}^0\|^4}{4\|\boldsymbol{\lambda}^*\|^2} \cdot \sin^2 2\omega_2. \quad (\text{trivial primal})$$

$$\|\boldsymbol{\zeta}^{k+1} - \boldsymbol{\zeta}^k\|^2 \leq \frac{1}{k+1} \cdot \|\boldsymbol{\zeta}^0\|^2 \cdot \sin^2 \omega_2. \quad (\text{fixed-point})$$

Proof. For case (i), Proposition 3.3 reduces to

$$\|\mathcal{A}\mathbf{x}^{k+2} - \mathcal{A}\mathbf{x}^{k+1}\|^2 \leq \frac{1}{k+1} \|\mathcal{A}\mathbf{x}^* + \frac{1}{\rho^2}\mathbf{0} - \frac{1}{\rho}\zeta^0\|^2. \quad (4.23)$$

Invoke the step-size choice ρ^* , which yields

$$\begin{aligned} \|\mathcal{A}\mathbf{x}^*\|^2 - \frac{2}{\rho^*} \langle \mathcal{A}\mathbf{x}^*, \zeta^0 \rangle + \frac{1}{(\rho^*)^2} \|\zeta^0\|^2 &= -\|\mathcal{A}\mathbf{x}^*\|^2 + \frac{\|\mathcal{A}\mathbf{x}^*\|^2}{\cos^2 \omega}, \\ &= \|\mathcal{A}\mathbf{x}^*\|^2 \tan^2 \omega_1. \end{aligned} \quad (4.24)$$

For the dual iterates, note that the primal and dual sequence rates are related via a factor of ρ^4 , recall Proposition 3.3. Hence,

$$\|\lambda^{k+1} - \lambda^k\|^2 \leq \frac{1}{k+1} \cdot (\rho^*)^4 \|\mathcal{A}\mathbf{x}^*\|^2 \tan^2 \omega, \quad (4.25)$$

$$= \frac{1}{k+1} \cdot \frac{\|\zeta^0\|^4}{\|\mathcal{A}\mathbf{x}^*\|^4} \cos^4 \omega_1 \cdot \|\mathcal{A}\mathbf{x}^*\|^2 \cdot \frac{\sin^2 \omega_1}{\cos^2 \omega_1}, \quad (4.26)$$

$$= \frac{1}{k+1} \cdot \frac{\|\zeta^0\|^4}{\|\mathcal{A}\mathbf{x}^*\|^2} \cdot \sin^2 \omega_1 \cos^2 \omega_1. \quad (4.27)$$

Invoke relation $\sin 2\omega_1 = 2 \sin \omega_1 \cos \omega_1$ yields the result. Similarly, the fixed-point admits a factor of ρ^2 relation to the primal, which gives

$$\|\zeta^{k+1} - \zeta^k\|^2 \leq \frac{1}{k+1} \cdot (\rho^*)^2 \|\mathcal{A}\mathbf{x}^*\|^2 \tan^2 \omega, \quad (4.28)$$

$$= \frac{1}{k+1} \cdot \frac{\|\zeta^0\|^2}{\|\mathcal{A}\mathbf{x}^*\|^2} \cos^2 \omega_1 \cdot \|\mathcal{A}\mathbf{x}^*\|^2 \cdot \frac{\sin^2 \omega_1}{\cos^2 \omega_1}, \quad (4.29)$$

$$= \frac{1}{k+1} \cdot \|\zeta^0\|^2 \cdot \sin^2 \omega_1. \quad (4.30)$$

At last, case (ii) is a symmetric situation and the same arguments apply, which are omitted to avoid repeating. The proof is now concluded. \square

Remarks 4.6 (good angle range: monotonic improvements). Recall from the previous section that the non-trivial sequence admits a fixed $1/(k+1)$ rate. Here, we see that such a rate is improved if

$$\tan^2 \omega < 1, \quad (4.31)$$

which corresponds to $\omega \in (-\pi/4, \pi/4) \cup (3\pi/4, 5\pi/4)$. Meanwhile, suppose ω is moving from (i) $-\pi/4$ towards 0, or (ii) from $\pi/4$ towards 0, or (iii) from $3\pi/4$ towards π , or (iv) from $5\pi/4$ towards π .

Then, we have $\tan^2 \omega$, $\sin^2 2\omega$, and $\sin^2 \omega$ monotonically decreasing, implying the rate bounds in Proposition 4.3 are monotonically improving.

The above result is optimal for the fixed-point sequence, which is a balance of primal and dual rates. However, for the partly trivial settings here, it appears that we do not need a balance. Instead, it seems natural to promote the non-trivial one as much as possible, meanwhile completely ignore the rest. This leads to the result below.

Proposition 4.4 (non-trivial sequence only). (i) Suppose $\|\mathcal{A}\mathbf{x}^*\| \neq 0$, $\|\boldsymbol{\lambda}^*\| = 0$. Set any initialization $\boldsymbol{\zeta}^0 \neq \mathbf{0}$. Let

$$\omega_1 = \arccos \frac{\langle \mathcal{A}\mathbf{x}^*, \boldsymbol{\zeta}^0 \rangle}{\|\mathcal{A}\mathbf{x}^*\| \|\boldsymbol{\zeta}^0\|}. \quad (\text{initial angle})$$

Choose step-size to be $\rho_{\text{pri}}^* = \frac{\|\boldsymbol{\zeta}^0\|}{\|\mathcal{A}\mathbf{x}^*\|} \frac{1}{\cos \omega_1}$. Then,

$$\|\mathcal{A}\mathbf{x}^{k+2} - \mathcal{A}\mathbf{x}^{k+1}\|^2 \leq \frac{1}{k+1} \cdot \|\mathcal{A}\mathbf{x}^*\|^2 \cdot \sin^2 \omega_1, \quad (\text{non-trivial})$$

$$\|\boldsymbol{\lambda}^{k+1} - \boldsymbol{\lambda}^k\|^2 \leq \frac{1}{k+1} \cdot \frac{\|\boldsymbol{\zeta}^0\|^4}{\|\mathcal{A}\mathbf{x}^*\|^2} \cdot \frac{\tan^2 \omega_1}{\cos^2 \omega_1}, \quad (\text{trivial dual})$$

$$\|\boldsymbol{\zeta}^{k+1} - \boldsymbol{\zeta}^k\|^2 \leq \frac{1}{k+1} \cdot \|\boldsymbol{\zeta}^0\|^2 \cdot \tan^2 \omega_1. \quad (\text{fixed-point})$$

(ii) Suppose $\|\mathcal{A}\mathbf{x}^*\| = 0$, $\|\boldsymbol{\lambda}^*\| \neq 0$. Set any initialization $\boldsymbol{\zeta}^0 \neq \mathbf{0}$. Let

$$\omega_2 = \arccos \frac{\langle \boldsymbol{\lambda}^*, \boldsymbol{\zeta}^0 \rangle}{\|\boldsymbol{\lambda}^*\| \|\boldsymbol{\zeta}^0\|}. \quad (\text{initial angle})$$

Choose step-size to be $\rho_{\text{dual}}^* = 1 / \left(\frac{\|\boldsymbol{\zeta}^0\|}{\|\boldsymbol{\lambda}^*\|} \frac{1}{\cos \omega_2} \right)$. Then,

$$\|\boldsymbol{\lambda}^{k+1} - \boldsymbol{\lambda}^k\|^2 \leq \frac{1}{k+1} \cdot \|\boldsymbol{\lambda}^*\|^2 \cdot \sin^2 \omega_2, \quad (\text{non-trivial})$$

$$\|\mathcal{A}\mathbf{x}^{k+2} - \mathcal{A}\mathbf{x}^{k+1}\|^2 \leq \frac{1}{k+1} \cdot \frac{\|\boldsymbol{\zeta}^0\|^4}{\|\boldsymbol{\lambda}^*\|^2} \cdot \frac{\tan^2 \omega_2}{\cos^2 \omega_2}, \quad (\text{trivial primal})$$

$$\|\boldsymbol{\zeta}^{k+1} - \boldsymbol{\zeta}^k\|^2 \leq \frac{1}{k+1} \cdot \|\boldsymbol{\zeta}^0\|^2 \cdot \tan^2 \omega_2. \quad (\text{fixed-point})$$

Proof. For case (i), Proposition 3.3 reduces to

$$\|\mathcal{A}\mathbf{x}^{k+2} - \mathcal{A}\mathbf{x}^{k+1}\|^2 \leq \frac{1}{k+1} \|\mathcal{A}\mathbf{x}^* + \frac{1}{\rho^2} \mathbf{0} - \frac{1}{\rho} \boldsymbol{\zeta}^0\|^2. \quad (4.32)$$

Hence, the step-size that optimize the above bound is

$$\rho_{\text{pri}}^* = \operatorname{argmin}_{\rho \neq 0} \|\mathcal{A}\mathbf{x}^* + \mathbf{0} - \frac{1}{\rho} \boldsymbol{\zeta}^0\|^2 = \|\boldsymbol{\zeta}^0\|^2 / \langle \mathcal{A}\mathbf{x}^*, \boldsymbol{\zeta}^0 \rangle = \|\boldsymbol{\zeta}^0\| / (\|\mathcal{A}\mathbf{x}^*\| \cos \omega_1). \quad (4.33)$$

The rest arguments are identical to Proposition 4.3, and are omitted to avoid repeating. The proof is now concluded. \square

Remarks 4.7 (comparison: improvement). Compare the above to the previous fixed-point view as in Proposition 4.3. We see that the non-trivial sequence convergence rate is guaranteed improved:

$$\tan^2 \omega \in [0, +\infty] \geq \sin^2 \omega \in [0, 1]. \quad (4.34)$$

Moreover, the upper rate bound is now guaranteed no worse than $1/(k+1)$, i.e., no worse than the previous zero-initialization case. The worst case happens if and only if either $\omega = \pi/2$, or $\omega = 3\pi/2$, i.e., when the initialization angle happens to be orthogonal to the ground-truth.

Remarks 4.8 (cost). The above improvement comes with a cost — an additional factor $1/\cos^6 \omega$ for the trivial iterate sequence, and factor $1/\cos^2 \omega$ for the fixed-point sequence.

Remarks 4.9 (optimal initialization preview). For all rate results in this section, the upper bounds take value 0 when $\omega = 0$ or $\omega = \pi$. This is the optimal initialization, and will be discussed below in a more general context.

4.4 Warm start: quality-based initial step-sizes

Across all previous sections, we see that the initialization makes a significant contribution to the convergence rate, meanwhile can be arbitrarily chosen. Then, a natural question is — what is the optimal choice?

This question needs to be answered separately: (i) for the primal and dual iterates, there is no extra freedom, and the optimal initialization is the optimal solution itself, i.e., a unique choice $\mathbf{x}^0 = \mathbf{x}^*$, $\boldsymbol{\lambda}^0 = \boldsymbol{\lambda}^*$; (ii) for the fixed-point, there exists a perturbation freedom, i.e., any element from the following set is optimal:

$$\boldsymbol{\zeta}_{\text{opt}}^0 \in \{\rho_0 \mathcal{A} \mathbf{x}^* + \boldsymbol{\lambda}^* / \rho_0 \mid \rho_0 \in [-\infty, +\infty] / \{0\}\}, \quad (4.35)$$

where ρ_0 is the initial step-size.

Despite all $\rho_0 \in [-\infty, +\infty] / \{0\}$ are equivalent in the above optimal case, they do make a difference in practice regarding the warm-start (not exactly optimal). Below, we provide a rough estimation to guide the initial step-size selection. In case that an estimation is not possible, we set $\rho_0 = 1$.

Proposition 4.5 (warm-start initial step-size). *Given a warm start as*

$$\mathbf{x}^0 = \mathbf{x}^* + \epsilon_{\text{err}1}, \quad \boldsymbol{\lambda}^0 = \boldsymbol{\lambda}^* + \epsilon_{\text{err}2}. \quad (4.36)$$

Let

$$\eta = \arccos \frac{\langle \mathcal{A} \epsilon_{\text{err}1}, \epsilon_{\text{err}2} \rangle}{\|\mathcal{A} \epsilon_{\text{err}1}\| \|\epsilon_{\text{err}2}\|}. \quad (4.37)$$

Fix the step-size to be:

$$\rho_k = \rho_0 = \pm \sqrt{\frac{\|\epsilon_{\text{err}2}\|}{\|\mathcal{A} \epsilon_{\text{err}1}\|}}, \quad \forall k = 1, 2, \dots \quad (4.38)$$

Then, the following hold:

$$\frac{\|\mathcal{A} \mathbf{x}^{k+2} - \mathcal{A} \mathbf{x}^{k+1}\|^2}{\|\mathcal{A} \epsilon_{\text{err}1}\|^2} \leq \frac{2}{k+1} (1 + \cos \eta), \quad (4.39)$$

$$\frac{\|\boldsymbol{\lambda}^{k+1} - \boldsymbol{\lambda}^k\|^2}{\|\epsilon_{\text{err}2}\|^2} \leq \frac{2}{k+1} (1 + \cos \eta), \quad (4.40)$$

$$\frac{\|\boldsymbol{\zeta}^{k+1} - \boldsymbol{\zeta}^k\|^2}{\|\mathcal{A} \epsilon_{\text{err}1}\| \|\epsilon_{\text{err}2}\|} \leq \frac{2}{k+1} (1 + \cos \eta). \quad (4.41)$$

Proof. The proof follows straightforwardly from Proposition 3.3. \square

Remarks 4.10 (quality-based initial choice). In view of (4.38), it is a norm ratio, and hence possible to be roughly estimated. This result can be interpreted as — one may choose the initial step-size based on the expected quality of the primal and dual warm-starts. The default choice can be $\rho_0 = 1$, implying no a priori knowledge at all.

Remarks 4.11 (warm start specification). Above, we did not specify how to achieve a warm start, due to it being a separate issue. As aforementioned, this issue has been intensively studied in the literature, see e.g. [12, 13].

4.5 Practical use

In the previous sections, we have established the theoretical optimal step-size selection principle. However, it is built on the optimal solutions, which are not known a priori. For practical use, we may replace the optimal solutions with the $(k + 1)$ -th iterate information and update the step-size adaptively, i.e., solve the following polynomial instead of (4.11):

$$\rho^4 \|\mathcal{A}\mathbf{x}^{k+1}\|^2 - \rho^3 \langle \mathcal{A}\mathbf{x}^{k+1}, \boldsymbol{\zeta}^0 \rangle + \rho \langle \boldsymbol{\lambda}^{k+1}, \boldsymbol{\zeta}^0 \rangle - \|\boldsymbol{\lambda}^{k+1}\|^2 = 0, \quad \rho \neq 0. \quad (4.42)$$

Let $\boldsymbol{\zeta}^0 = \mathbf{0}$, we obtain a simple version:

Algorithm 2 ADMM with adaptive step-sizes (zero initialization)

Input: Set $\mathbf{z}^0 = \mathbf{0}$, $\boldsymbol{\lambda}^0 = \mathbf{0}$, $\rho_0 = 1$.

1: **while** iteration $k = 0, 1, 2, \dots$ **do**

2:

$$\mathbf{x}^{k+1} = \underset{\mathbf{x}}{\operatorname{argmin}} f(\mathbf{x}) + \frac{1}{2} \|\rho_k(\mathcal{A}\mathbf{x} - \mathcal{B}\mathbf{z}^k - \mathbf{c}) + \boldsymbol{\lambda}^k / \rho_k\|^2, \quad (4.43)$$

$$\mathbf{z}^{k+1} = \underset{\mathbf{z}}{\operatorname{argmin}} g(\mathbf{z}) + \frac{1}{2} \|\rho_k(\mathcal{A}\mathbf{x}^{k+1} - \mathcal{B}\mathbf{z} - \mathbf{c}) + \boldsymbol{\lambda}^k / \rho_k\|^2, \quad (4.44)$$

$$\boldsymbol{\lambda}^{k+1} = \boldsymbol{\lambda}^k + (\rho_k)^2 (\mathcal{A}\mathbf{x}^{k+1} - \mathcal{B}\mathbf{z}^{k+1} - \mathbf{c}), \quad (4.45)$$

$$\rho_{k+1} = \pm \sqrt{\|\boldsymbol{\lambda}^{k+1}\| / \|\mathbf{x}^{k+1}\|} \quad // \text{ two choices are equivalent.} \quad (4.46)$$

3: **end while**

Output: primal and dual solutions \mathbf{x}^* and $\boldsymbol{\lambda}^*$, respectively.

If one can access a good $\boldsymbol{\zeta}^0$, then the following version may be employed:

Algorithm 3 ADMM with adaptive step-sizes (warm start)

Input: Iterates warm-start $\boldsymbol{\lambda}^0 \in \mathbb{K}$, $\boldsymbol{z}^0 \in \mathbb{P}$. Initial step-size ρ_0 by estimating (4.38) (if not feasible, set $\rho_0 = 1$). Let $\mathcal{A}\boldsymbol{x}^0 = \mathcal{B}\boldsymbol{z}^0 + \boldsymbol{c}$ and let $\boldsymbol{\zeta}^0 = \rho_0\mathcal{A}\boldsymbol{x}^0 + \boldsymbol{\lambda}^0/\rho_0$.

1: **while** iteration $k = 0, 1, 2, \dots$ **do**
2:

$$\begin{aligned}\boldsymbol{x}^{k+1} &= \underset{\boldsymbol{x}}{\operatorname{argmin}} f(\boldsymbol{x}) + \frac{1}{2}\|\rho_k(\mathcal{A}\boldsymbol{x} - \mathcal{B}\boldsymbol{z}^k - \boldsymbol{c}) + \boldsymbol{\lambda}^k/\rho_k\|^2, \\ \boldsymbol{z}^{k+1} &= \underset{\boldsymbol{z}}{\operatorname{argmin}} g(\boldsymbol{z}) + \frac{1}{2}\|\rho_k(\mathcal{A}\boldsymbol{x}^{k+1} - \mathcal{B}\boldsymbol{z} - \boldsymbol{c}) + \boldsymbol{\lambda}^k/\rho_k\|^2, \\ \boldsymbol{\lambda}^{k+1} &= \boldsymbol{\lambda}^k + (\rho_k)^2(\mathcal{A}\boldsymbol{x}^{k+1} - \mathcal{B}\boldsymbol{z}^{k+1} - \boldsymbol{c}).\end{aligned}\tag{4.47}$$

3: Compute the $(k+1)$ -th step-size choice $\rho_{k+1} \neq 0$ as a root of

$$\rho^4\|\mathcal{A}\boldsymbol{x}^{k+1}\|^2 - \rho^3\langle\mathcal{A}\boldsymbol{x}^{k+1}, \boldsymbol{\zeta}^0\rangle + \rho\langle\boldsymbol{\lambda}^{k+1}, \boldsymbol{\zeta}^0\rangle - \|\boldsymbol{\lambda}^{k+1}\|^2 = 0,\tag{4.48}$$

with a closed-form expression specified in Sec. 4.2.1.

4: **end while**

Output: primal and dual solutions \boldsymbol{x}^* and $\boldsymbol{\lambda}^*$, respectively.

Remarks 4.12 (adaptive convergence). Numerically, we find that the above two algorithms always converge in all our experiments. By a closer look, we find that the convergence owes to that the adaptive step-size will soon converge to the fixed optimal step-size.

Theoretically, we may establish convergence by adding a criterion to force the algorithm stop updating the step-size after some iterations. Then, the ADMM convergence result for a fixed step-size can apply, see Proposition 2.5. (Meanwhile, such an early stop can save some runtime.)

Remarks 4.13 (literature connection). The above adaptive estimation of the optimal point information has been successfully applied in the importance sampling from the machine learning field, see [35, Sec. IV. C], [36].

Remarks 4.14 (non-trivial only view). The above is a balanced/fixed-point view. Similar adaptive strategy also applies to the partly trivial case in Proposition 4.4. For example, consider its non-trivial primal case (i). Let $\omega_1^k = \arccos \langle \mathcal{A}\boldsymbol{x}^k, \boldsymbol{\zeta}^0 \rangle / (\|\mathcal{A}\boldsymbol{x}^k\| \|\boldsymbol{\zeta}^0\|)$. Then, adaptively set $\rho_k = \|\boldsymbol{\zeta}^0\| / (\|\mathcal{A}\boldsymbol{x}^k\| \cos \omega_1^k)$. Same arguments apply to dual case (ii). See numerical details in Sec. 5.2.2.

5 Numerical examples

Below, we test our results via two numerical examples. For the general non-trivial case, we consider the popular Lasso application; for the partly trivial case, we study the feasibility problem.

5.1 Lasso

Consider the following problem:

$$\text{minimize } \frac{1}{2} \|\mathbf{A}\mathbf{x} - \mathbf{b}\|^2 + \alpha \|\mathbf{z}\|_1, \quad \text{subject to } \mathbf{x} = \mathbf{z}. \quad (5.1)$$

with variable $\mathbf{x} \in \mathbb{R}^{1000}$, $\mathbf{b} \in \mathbb{R}^{300}$, $\mathbf{A} \in \mathbb{R}^{300 \times 1000}$. We generate elements of \mathbf{A}, \mathbf{x} from a normal distribution $\mathcal{N}(0, 1)$. We set $\mathbf{b} = \mathbf{A}\mathbf{x}_0 + \epsilon_{\text{noise}}$, where \mathbf{x}_0 is a random sparse vector, with density factor 1/3, and where ϵ_{noise} is some random noise from $\mathcal{N}(0, 0.1)$. At last, we set regularization parameter $\alpha = 0.1 \|\mathbf{A}^T \mathbf{b}\|_\infty$.

Unless specified, the figures are plotted against the following normalized error measures:

$$\frac{\|\zeta^{k+1} - \zeta^k\|^2}{\|\mathbf{x}^* \|^2 \|\boldsymbol{\lambda}^* \|^2}, \quad \frac{\|\mathbf{x}^{k+2} - \mathbf{x}^{k+1}\|^2}{\|\mathbf{x}^* \|^2}, \quad \frac{\|\boldsymbol{\lambda}^{k+1} - \boldsymbol{\lambda}^k\|^2}{\|\boldsymbol{\lambda}^* \|^2}. \quad (\text{normalized errors})$$

Remarks 5.1 (data conditioning). Above, we did not apply column-normalization for the sensing matrix \mathbf{A} . We find that if normalized, the optimal choice ρ^* is roughly at ± 0.9 , i.e., close to the unit length, implying the data is originally well-conditioned, where the step-size selection becomes less important.

5.1.1 zero initialization

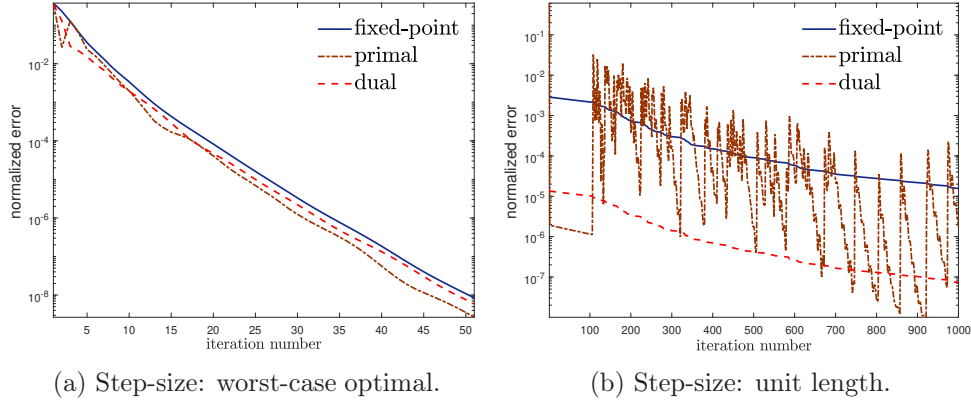


Figure 1: (Fixed step-size) Theoretical results, see Proposition 4.1.

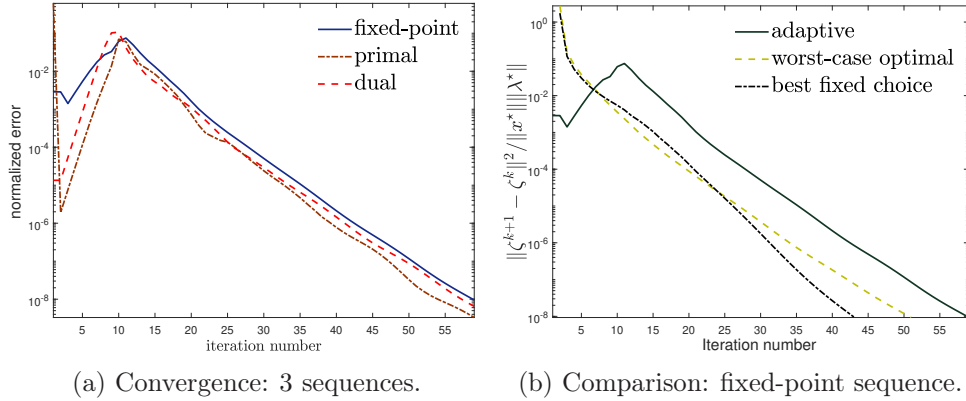


Figure 2: (Adaptive step-size) Practical use via Algorithm 2.

Remarks 5.2 (balanced rates). The above numerical results do align with our theoretical conclusions — the optimal step-size would set all sequences (fixed-point, primal and dual) to the same speed.

Remarks 5.3 (adaptive). Compare Fig. 2a and Fig. 1a, we see that the adaptive strategy performs quite differently at the beginning stage, but soon (roughly 13 iterations) becomes stable and similar to the theoretical one.

Remarks 5.4 (near-limit performance). In Fig. 2b, we investigate how much potential is left for further improvement, since ours is only optimal in the worst-case sense (no tailored structure exploited). To this end, we fixed the random number generator with seed 0, and found the underlying best fixed step-size choice via an exhaustive grid search. Quite remarkably, we see that our choice is similar to the underlying best fixed one.

5.1.2 warm start

Here, we test the warm start case corresponding to Sec. 4.4 with settings: (i) Full warm-start: $\mathbf{x}^0 = \mathbf{x}^* + \epsilon_{\text{err}1}$, $\boldsymbol{\lambda}^0 = \boldsymbol{\lambda}^* + \epsilon_{\text{err}2}$; (ii) Partial warm-start: $\mathbf{x}^0 = \mathbf{x}^* + \epsilon_{\text{err}1}$, $\boldsymbol{\lambda}^0 = \mathbf{0}$; (iii) Random initialization: $\mathbf{x}^0 \sim \mathcal{N}(0, 1)$, $\boldsymbol{\lambda}^0 \sim \mathcal{N}(0, 1)$.

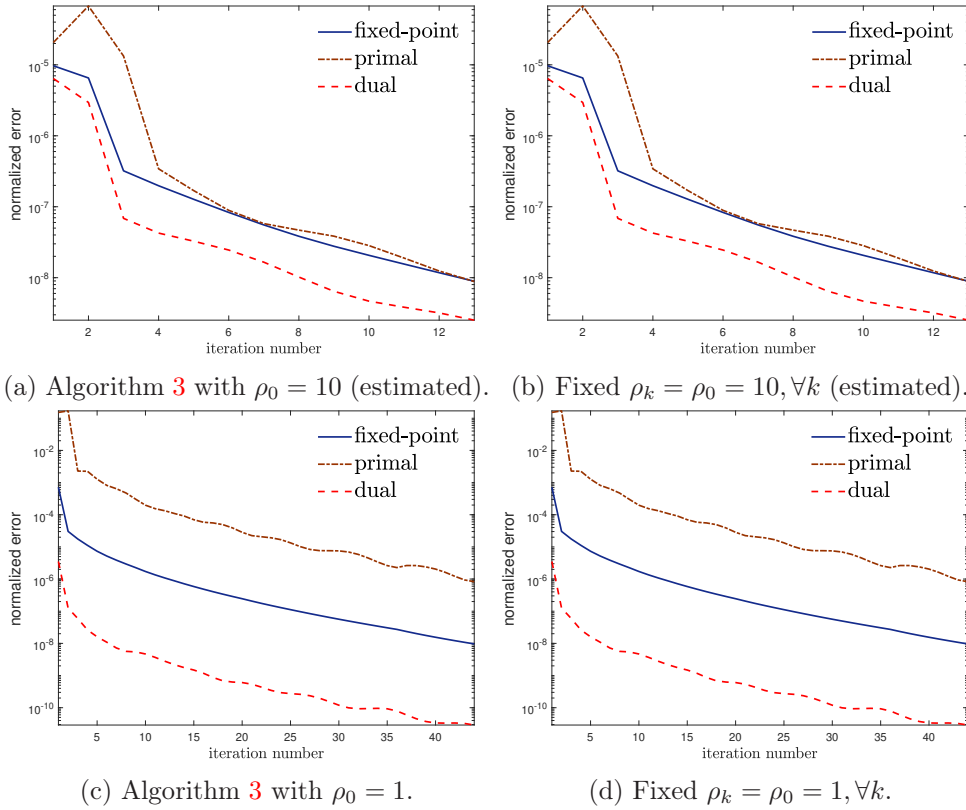


Figure 3: Full warm-start with $\epsilon_{\text{err}1} \sim \mathcal{N}(0, 10^{-3})$, $\epsilon_{\text{err}2} \sim \mathcal{N}(0, 10^{-1})$.

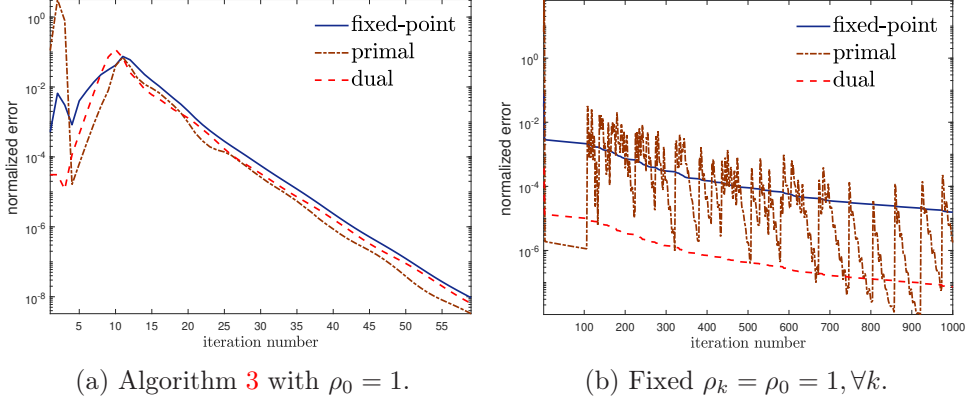


Figure 4: Partial warm-start with $\epsilon_{\text{err}1} \sim \mathcal{N}(0, 1)$.

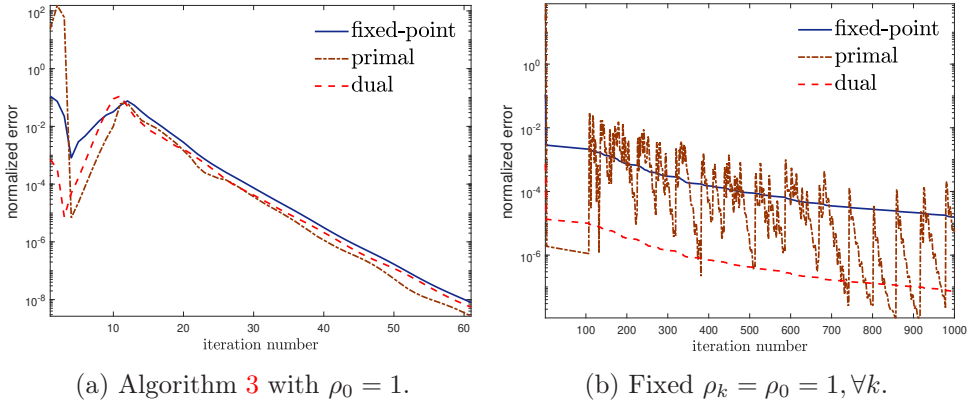


Figure 5: Random initialization: $\mathbf{x}^0 \sim \mathcal{N}(0, 1)$, $\boldsymbol{\lambda}^0 \sim \mathcal{N}(0, 1)$.

Remarks 5.5 (full warm start). In view of Fig. 3, our Algorithm 3 is roughly identical to the fixed step-size strategy. By a closer look, we find that our adaptive step-size update in (4.48) outputs almost-identical value as ρ_0 . In fact, this is not too surprising by viewing (4.35). That is, given a full warm-start setting, the best fixed-point is likely the one corresponds to ρ_0 .

Additionally, due to the warm-start is not exactly optimal. We can change ρ_0 to accelerate certain sequences. Here, by $\rho_0 = 10$, we are promoting the fixed-point sequence rate, which is roughly $4\times$ faster than setting $\rho_0 = 1$.

Remarks 5.6 (other initializations). We see that our algorithm exhibits great advantages in Fig 4 and Fig 5, regarding partial warm start and random initialization, respectively.

Additionally, we omit the case $\mathbf{x}^0 = \mathbf{0}, \boldsymbol{\lambda}^0 = \boldsymbol{\lambda}^* + \epsilon_{\text{err}2}$, since for Lasso, the optimal primal \mathbf{x}^* is highly sparse, similar to a zero vector. We observe that such a setting is similar to the full warm start case.

5.2 Partly trivial: feasibility problem

Here, we consider a special application where the dual solution is trivial, i.e., a zero vector $\lambda^* = \mathbf{0}$. Consider the following feasibility problem:

$$\begin{aligned} & \text{Find } \mathbf{x} \in \mathbb{H}, \\ & \text{subject to } \mathbf{x} \in C, \\ & \mathbf{x} \in D, \end{aligned} \tag{5.2}$$

where subsets C, D are specified as

$$C = \{\mathbf{y} \in \mathbb{R}^{200} \mid \mathbf{A}_1 \mathbf{y} = \mathbf{b}_1\}, \quad D = \{\mathbf{z} \in \mathbb{R}^{200} \mid \mathbf{A}_2 \mathbf{z} = \mathbf{b}_2\}, \tag{5.3}$$

with $\mathbf{A}_1 \in \mathbb{R}^{80 \times 200}$, $\mathbf{b}_1 \in \mathbb{R}^{80}$, and $\mathbf{A}_2 \in \mathbb{R}^{100 \times 200}$, $\mathbf{b}_2 \in \mathbb{R}^{100}$.

It can be rewritten into an ADMM form:

$$\text{minimize } \mathbf{1}_C(\mathbf{x}) + \mathbf{1}_D(\mathbf{z}) \quad \text{subject to } \mathbf{x} = \mathbf{z}, \tag{5.4}$$

with $\mathbf{1}_C$ and $\mathbf{1}_D$ the indicator functions corresponding to (5.3).

The figures in this section are plotted against the following normalized error measures, corresponding to Proposition 4.1:

$$\|\zeta^{k+1} - \zeta^k\|^2, \quad \|\mathbf{x}^{k+2} - \mathbf{x}^{k+1}\|^2, \quad \|\lambda^{k+1} - \lambda^k\|^2. \quad (\text{error measures})$$

5.2.1 zero initialization: fixed non-trivial rate

For the above problem, set $\zeta^0 = \mathbf{0}$. Then, Proposition 4.2 reduces to:

$$\|\mathbf{x}^{k+2} - \mathbf{x}^{k+1}\|^2 \leq \frac{1}{k+1} \|\mathbf{x}^*\|^2, \quad (\text{primal})$$

$$\|\lambda^{k+1} - \lambda^k\|^2 \leq \frac{1}{k+1} \|\mathbf{x}^*\|^2 \cdot \rho^4, \quad (\text{trivial dual})$$

$$\|\zeta^{k+1} - \zeta^k\|^2 \leq \frac{1}{k+1} \|\mathbf{x}^*\|^2 \cdot \rho^2. \quad (\text{fixed-point})$$

Here, we numerically verify this result. For clarity, below we only plot the primal and fixed-point sequences.

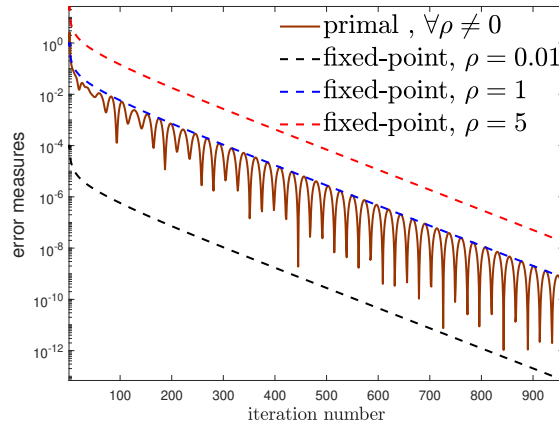


Figure 6: Fixed rate for primal iterate, independent of step-size choices.

Remarks 5.7. From above, we see that primal sequence (non-trivial) has exactly the same practical convergence rate, regardless of the step-size choices. Meanwhile, the fixed-point rate does improve as the step-size ρ approaching 0, which is aligned with the above theory (fixed-point).

5.2.2 non-zero initialization

For the above problem, set any $\zeta^0 \neq \mathbf{0}$. Let $\omega = \arccos \langle \mathbf{x}^*, \zeta^0 \rangle / \|\mathbf{x}^*\| \|\zeta^0\|$.

- (i) (balanced view) Set $\rho^* = \frac{\|\zeta^0\|}{\|\mathbf{x}^*\|} \cos \omega$. Then, Proposition 4.3 reduces to

$$\|\mathbf{x}^{k+2} - \mathbf{x}^{k+1}\|^2 \leq \frac{1}{k+1} \|\mathbf{x}^*\|^2 \cdot \tan^2 \omega, \quad (5.5)$$

- (ii) (non-trivial only) Set $\rho_{\text{pri}}^* = \frac{\|\zeta^0\|}{\|\mathbf{x}^*\|} \frac{1}{\cos \omega}$. Then, Proposition 4.4 gives

$$\|\mathbf{x}^{k+2} - \mathbf{x}^{k+1}\|^2 \leq \frac{1}{k+1} \|\mathbf{x}^*\|^2 \cdot \sin^2 \omega. \quad (5.6)$$

For practical use, let

$$\omega_{k+1} = \arccos \frac{\langle \mathbf{x}^{k+1}, \zeta^0 \rangle}{\|\mathbf{x}^{k+1}\| \|\zeta^0\|}, \quad k = 0, 1, \dots, \quad (5.7)$$

and adaptively update the step-size via

$$\rho_{k+1} = \frac{\|\zeta^0\|}{\|\mathbf{x}^{k+1}\|} \cdot \cos \omega_{k+1}, \quad (\text{balanced view})$$

$$\rho_{k+1} = \frac{\|\zeta^0\|}{\|\mathbf{x}^{k+1}\|} \cdot \frac{1}{\cos \omega_{k+1}}. \quad (\text{primal iterate view})$$

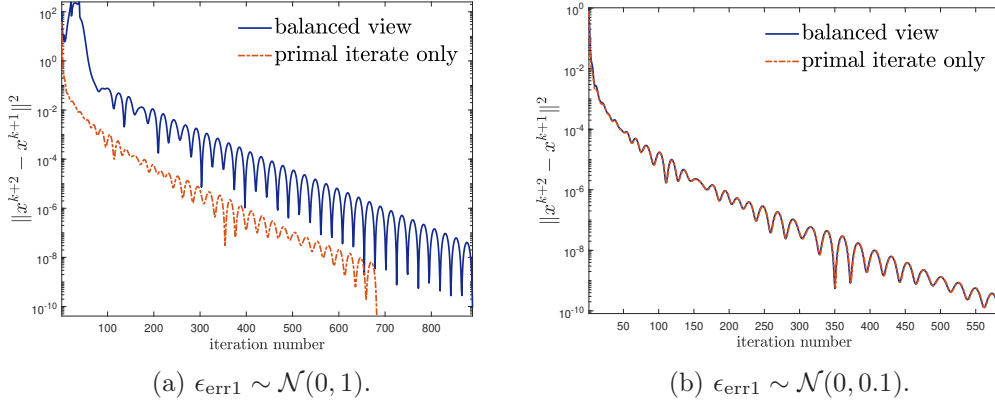


Figure 7: (Adaptive) Primal warm-start: $\mathbf{x}^0 = \mathbf{x}^* + \epsilon_{\text{err}1}$, $\lambda^0 = \mathbf{0}$.

Remarks 5.8. In view of (5.5) and (5.6), we see that the two worst-case rates admit a factor difference of $\cos^2 \omega$. (i) For Fig. 7a, we find $\cos^2 \omega \approx 0.023$. Theoretically, we expect different convergence rates, which is indeed the case numerically. (ii) For Fig. 7b, we find $\cos^2 \omega \approx 0.78$, which is close to 1, we expect them to be similar, and numerically they admit the same performance.

5.2.3 Comparison

Here, we make comparison between zero and non-zero initialization. We are motivated by the following theoretical results:

$$\begin{aligned}\|\mathbf{x}^{k+2} - \mathbf{x}^{k+1}\|^2 &\leq \frac{1}{k+1} \|\mathbf{x}^\star\|^2, & (\text{zero ini., see (primal)}) \\ \|\mathbf{x}^{k+2} - \mathbf{x}^{k+1}\|^2 &\leq \frac{1}{k+1} \|\mathbf{x}^\star\|^2 \cdot \sin^2 \omega. & (\text{non-zero ini., see (5.6)})\end{aligned}$$

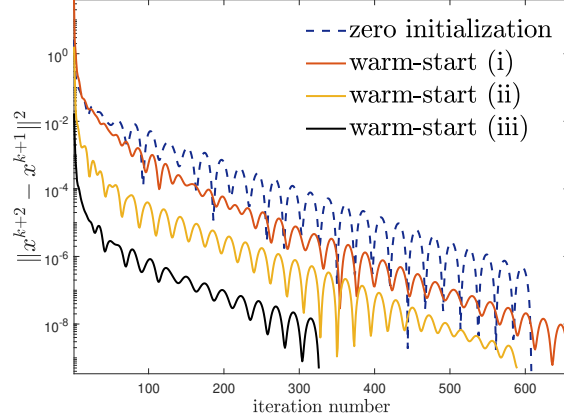


Figure 8: (Adaptive) Comparison: warm-start $\mathbf{x}^0 = \mathbf{x}^\star + \epsilon_{\text{err1}}$, $\lambda^0 = \mathbf{0}$, with (i) $\epsilon_{\text{err1}} \sim \mathcal{N}(0, 1)$; (ii) $\epsilon_{\text{err1}} \sim \mathcal{N}(0, 0.1)$; (iii) $\epsilon_{\text{err1}} \sim \mathcal{N}(0, 0.01)$.

Remarks 5.9. Numerically, the 3 warm-start settings above admit angle values: (i) $\sin^2 \omega \approx 0.98$; (ii) $\sin^2 \omega \approx 0.22$; (iii) $\sin^2 \omega \approx 0.003$. For a smaller $\sin^2 \omega$, we do observe an improved convergence rate, which aligns with the theoretical result.

6 Conclusion

In this work, we present a general, simple, worst-case optimal step-size selection principle for ADMM-type algorithms, which solves a long-standing open issue. There are two main types of choices: (i) step-size that accelerates the fixed-point sequence, which yields some balanced rates; (ii) accelerating only the primal or dual iterate, at the cost of slowing down all other sequences.

The key to our success owes to a novel domain-type parametrization, symmetric to the range-type in the current literature, which avoids an implicit step-size related scaling/shifting. Interestingly, we reveal that the algorithm's efficiency (optimal convergence rate) is intrinsically related to the primal-dual solution and initialization angles. This discovery appears useful and may be worth further investigation in the future.

References

- [1] Stephen Boyd, Neal Parikh, Eric Chu, Borja Peleato, Jonathan Eckstein, et al. Distributed optimization and statistical learning via the alternating direction method of multipliers. *Foundations and Trends® in Machine learning*, 3(1):1–122, 2011.
- [2] Roland Glowinski and Americo Marroco. Sur l’approximation, par éléments finis d’ordre un, et la résolution, par pénalisation-dualité d’une classe de problèmes de dirichlet non linéaires. *Revue française d’automatique, informatique, recherche opérationnelle. Analyse numérique*, 9(R2):41–76, 1975.
- [3] Daniel Gabay and Bertrand Mercier. A dual algorithm for the solution of nonlinear variational problems via finite element approximation. *Computers & mathematics with applications*, 2(1):17–40, 1976.
- [4] R Tyrrell Rockafellar. *Convex analysis*, volume 11. Princeton university press, 1997.
- [5] Stephen P Boyd and Lieven Vandenbergh. *Convex optimization*. Cambridge university press, 2004.
- [6] Bartolomeo Stellato, Goran Banjac, Paul Goulart, Alberto Bemporad, and Stephen Boyd. Osqp: An operator splitting solver for quadratic programs. *Mathematical Programming Computation*, 12(4):637–672, 2020.
- [7] Goran Banjac and Paul J Goulart. Tight global linear convergence rate bounds for operator splitting methods. *IEEE Transactions on Automatic Control*, 63(12):4126–4139, 2018.
- [8] Pontus Giselsson and Stephen Boyd. Linear convergence and metric selection for douglas-rachford splitting and admm. *IEEE Transactions on Automatic Control*, 62(2):532–544, 2016.
- [9] Ernest K Ryu and Wotao Yin. *Large-scale convex optimization: algorithms & analyses via monotone operators*. Cambridge University Press, 2022.
- [10] Yuxiao Chen, Mario Santillo, Mrdjan Jankovic, and Aaron D Ames. Online decentralized decision making with inequality constraints: an admm approach. *IEEE Control Systems Letters*, 5(6):2156–2161, 2020.
- [11] Jianbo Ye and Jia Li. Scaling up discrete distribution clustering using admm. In *2014 IEEE International Conference on Image Processing (ICIP)*, pages 5267–5271. IEEE, 2014.
- [12] Rajiv Sambharya, Georgina Hall, Brandon Amos, and Bartolomeo Stellato. End-to-end learning to warm-start for real-time quadratic optimization. In *Learning for Dynamics and Control Conference*, pages 220–234. PMLR, 2023.
- [13] Rajiv Sambharya, Georgina Hall, Brandon Amos, and Bartolomeo Stellato. Learning to warm-start fixed-point optimization algorithms. *arXiv preprint arXiv:2309.07835*, 2023.

- [14] Terrence WK Mak, Minas Chatzos, Mathieu Tanneau, and Pascal Van Hentenryck. Learning regionally decentralized ac optimal power flows with admm. *IEEE Transactions on Smart Grid*, 2023.
- [15] Jim Douglas and Henry H Rachford. On the numerical solution of heat conduction problems in two and three space variables. *Transactions of the American mathematical Society*, 82(2):421–439, 1956.
- [16] Jonathan Eckstein and Dimitri P Bertsekas. On the Douglas—Rachford splitting method and the proximal point algorithm for maximal monotone operators. *Mathematical Programming*, 55(1):293–318, 1992.
- [17] Michel Fortin and Roland Glowinski. *Augmented Lagrangian methods: applications to the numerical solution of boundary-value problems*. Elsevier, 2000.
- [18] Daniel O’Connor and Lieven Vandenbergh. On the equivalence of the primal-dual hybrid gradient method and Douglas–Rachford splitting. *Mathematical Programming*, 179(1):85–108, 2020.
- [19] Antonin Chambolle and Thomas Pock. A first-order primal-dual algorithm for convex problems with applications to imaging. *Journal of mathematical imaging and vision*, 40(1):120–145, 2011.
- [20] Ernie Esser, Xiaoqun Zhang, and Tony F Chan. A general framework for a class of first order primal-dual algorithms for convex optimization in imaging science. *SIAM Journal on Imaging Sciences*, 3(4):1015–1046, 2010.
- [21] Thomas Pock, Daniel Cremers, Horst Bischof, and Antonin Chambolle. An algorithm for minimizing the Mumford-Shah functional. In *2009 IEEE 12th International Conference on Computer Vision*, pages 1133–1140. IEEE, 2009.
- [22] Clarice Poon and Jingwei Liang. Trajectory of alternating direction method of multipliers and adaptive acceleration. *Advances in Neural Information Processing Systems*, 32, 2019.
- [23] Neal Parikh and Stephen Boyd. Proximal algorithms. *Foundations and Trends in optimization*, 1(3):127–239, 2014.
- [24] Jean-Jacques Moreau. Proximité et dualité dans un espace hilbertien. *Bulletin de la Société mathématique de France*, 93:273–299, 1965.
- [25] Euhanna Ghadimi, André Teixeira, Iman Shames, and Mikael Johansson. Optimal parameter selection for the alternating direction method of multipliers (ADMM): quadratic problems. *IEEE Transactions on Automatic Control*, 60(3):644–658, 2014.
- [26] Wei Shi, Qing Ling, Kun Yuan, Gang Wu, and Wotao Yin. On the linear convergence of the admm in decentralized consensus optimization. *IEEE Transactions on Signal Processing*, 62(7):1750–1761, 2014.
- [27] Heinz H Bauschke and Patrick L Combettes. *Convex Analysis and Monotone Operator Theory in Hilbert Spaces*. Springer, 2017.

- [28] Radu Ioan Boţ and Ernő Robert Csetnek. Admm for monotone operators: convergence analysis and rates. *Advances in Computational Mathematics*, 45:327–359, 2019.
- [29] Ron Shefi and Marc Teboulle. Rate of convergence analysis of decomposition methods based on the proximal method of multipliers for convex minimization. *SIAM Journal on Optimization*, 24(1):269–297, 2014.
- [30] Sebastian Banert, Radu Ioan Boţ, and Ernő Robert Csetnek. Fixing and extending some recent results on the admm algorithm. *Numerical Algorithms*, 86:1303–1325, 2021.
- [31] Walaa M Moursi and Lieven Vandenbergh. Douglas–rachford splitting for the sum of a lipschitz continuous and a strongly monotone operator. *Journal of Optimization Theory and Applications*, 183:179–198, 2019.
- [32] Bingsheng He and Xiaoming Yuan. On non-ergodic convergence rate of Douglas–Rachford alternating direction method of multipliers. *Numerische Mathematik*, 130(3):567–577, 2015.
- [33] Bing-Sheng He, Hai Yang, and SL Wang. Alternating direction method with self-adaptive penalty parameters for monotone variational inequalities. *Journal of Optimization Theory and applications*, 106:337–356, 2000.
- [34] SL Wang and LZ Liao. Decomposition method with a variable parameter for a class of monotone variational inequality problems. *Journal of optimization theory and applications*, 109:415–429, 2001.
- [35] Elsa Rizk, Stefan Vlaski, and Ali H. Sayed. Federated learning under importance sampling. *IEEE Transactions on Signal Processing*, 70:5381–5396, 2022.
- [36] Kun Yuan, Bicheng Ying, Stefan Vlaski, and Ali H. Sayed. Stochastic gradient descent with finite samples sizes. In *2016 IEEE 26th International Workshop on Machine Learning for Signal Processing (MLSP)*, pages 1–6, 2016.

A Additional experiments

This material aims to support the generality claim of our step-size selection scheme. All experiments below use the standard data settings from the review paper by Stephen Boyd et al. [1], with open-sourced code from their website (relatively well-conditioned data).

All figures in this section are plotted against the following measures (unless specified), which we referred to as the normalized errors:

$$\frac{\|\zeta^{k+1} - \zeta^k\|^2}{\|\mathcal{A}\mathbf{x}^*\| \|\boldsymbol{\lambda}^*\|}, \quad \frac{\|\mathcal{A}\mathbf{x}^{k+2} - \mathcal{A}\mathbf{x}^{k+1}\|^2}{\|\mathcal{A}\mathbf{x}^*\|^2}, \quad \frac{\|\boldsymbol{\lambda}^{k+1} - \boldsymbol{\lambda}^k\|^2}{\|\boldsymbol{\lambda}^*\|^2}. \quad (\text{A.1})$$

For non-zero initialization, we test the following settings:

- (i) Full warm-start: $\mathbf{x}^0 = \mathbf{x}^* + \epsilon_{\text{err}1}$, $\boldsymbol{\lambda}^0 = \boldsymbol{\lambda}^* + \epsilon_{\text{err}2}$;
- (ii) Partial primal warm-start: $\mathbf{x}^0 = \mathbf{x}^* + \epsilon_{\text{err}1}$, $\boldsymbol{\lambda}^0 = \mathbf{0}$;
- (iii) Partial dual warm-start: $\mathbf{x}^0 = \mathbf{0}$, $\boldsymbol{\lambda}^0 = \boldsymbol{\lambda}^* + \epsilon_{\text{err}2}$.
- (iv) Random initialization: $\mathbf{x}^0 \sim \mathcal{N}(0, 1)$, $\boldsymbol{\lambda}^0 \sim \mathcal{N}(0, 1)$.

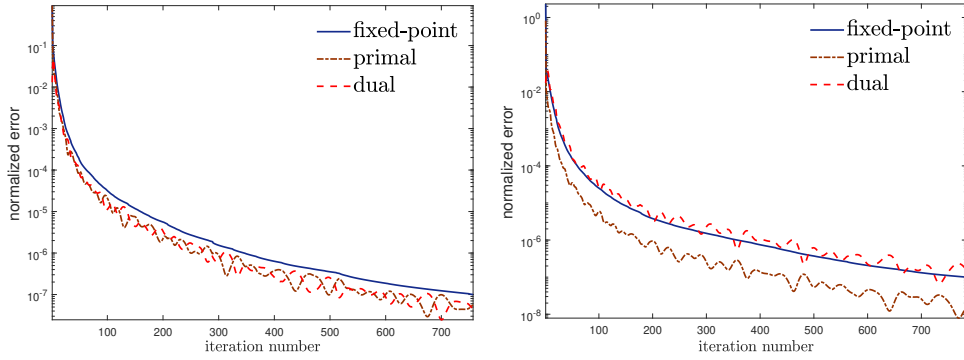
A.1 Linear programming

Consider the following linear program:

$$\text{minimize } \mathbf{c}^T \mathbf{x} \quad \text{subject to } \mathbf{A}\mathbf{x} = \mathbf{b}, \mathbf{x} \geq 0, \quad (\text{A.2})$$

with variable $\mathbf{x}, \mathbf{c} \in \mathbb{R}^{500}, \mathbf{b} \in \mathbb{R}^{400}, \mathbf{A} \in \mathbb{R}^{400 \times 500}$. Vector \mathbf{c} is generated from a uniform distribution on interval $[0.5, 1.5]$. The elements of \mathbf{x}, \mathbf{A} are generated from a normal distribution $\mathcal{N}(0, 1)$ and then set to be positive by taking the absolute value. \mathbf{b} is set equal to $\mathbf{A}\mathbf{x}$.

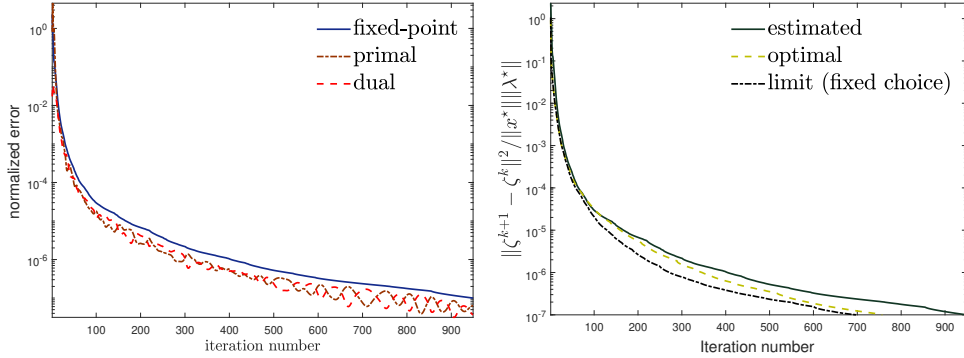
A.1.1 zero initialization



(a) Step-size: optimal choice $\rho^* \approx \pm 0.6$.

(b) Step-size: unit length.

Figure 9: Theoretical results test (zero initialization).



(a) Estimated step-size choice (adaptive).

(b) Fixed-point convergence comparison.

Figure 10: Practical use test (adaptive; zero initialization).

Remarks A.1. The above two step-size choices exhibit similar performances. With a closer look, we find that the optimal choice in Fig. 9a does yield a marginally faster fixed-point sequence convergence (requires 754 iterations, compared to 778). Meanwhile, its primal iterates convergence is slightly slower than the unit-length step-size.

Remarks A.2. We see that the adaptive step-size does well-approximate the previous theoretical result, and exhibits near-limit (for fixed step-size) performance.

A.1.2 non-zero initialization

Set non-zero $\zeta^0 \neq \mathbf{0}$ according to the 4 strategies at the beginning of the appendix.

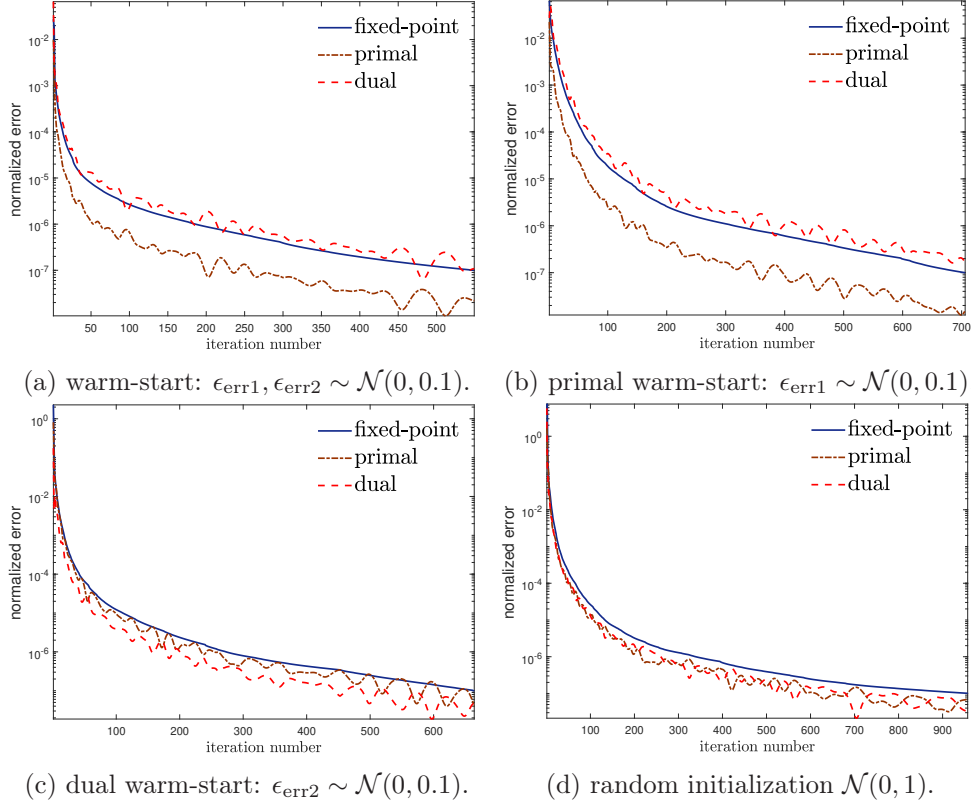


Figure 11: Practical use test (adaptive, $\rho_0 = 1$).

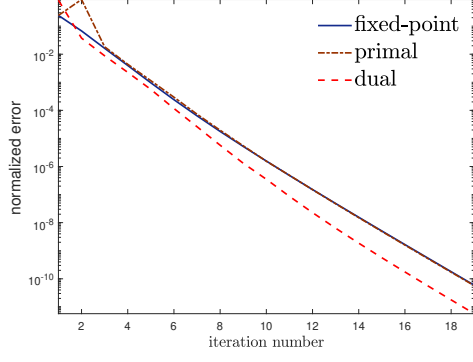
Remarks A.3. Compared the above to the previous zero initialization case, we see that a warm start does improve the performance. Interestingly, random initialization exhibits a similar performance compared to Fig. 10a.

A.2 Quadratic programming

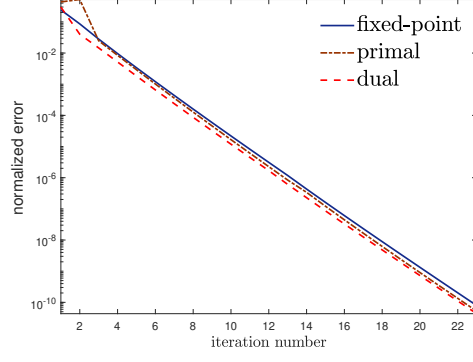
Consider the following quadratic program:

$$\text{minimize } \frac{1}{2} \mathbf{x}^T \mathbf{P} \mathbf{x} + \mathbf{q}^T \mathbf{x} + r \quad \text{subject to } \mathbf{a} \leq \mathbf{x} \leq \mathbf{b}, \quad (\text{A.3})$$

with variable $r \in \mathbb{R}$, $\mathbf{x}, \mathbf{q} \in \mathbb{R}^{100}$, $\mathbf{P} \in \mathbb{S}_{++}^{100}$ (positive definite matrix). The elements of \mathbf{P} are first generated from a uniform distribution on interval $[0, 1]$. Then, its eigenvalues are increased by a uniformly distributed random number from $[0, 1]$. All other data is generated from $\mathcal{N}(0, 1)$.

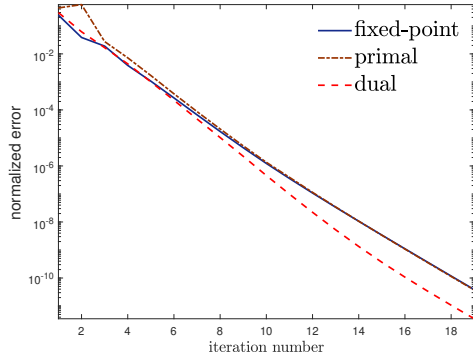


(a) Step-size: optimal choice $\rho^* \approx \pm 1.34$.

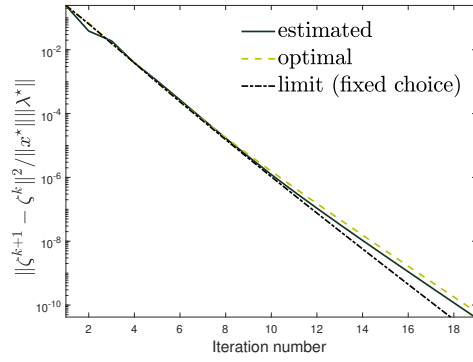


(b) Step-size: unit length.

Figure 12: Theoretical results test (zero initialization).

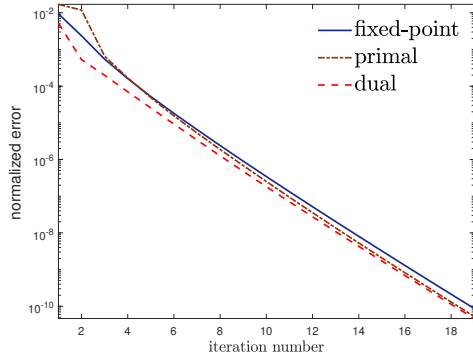


(a) Estimated step-size choice (adaptive).

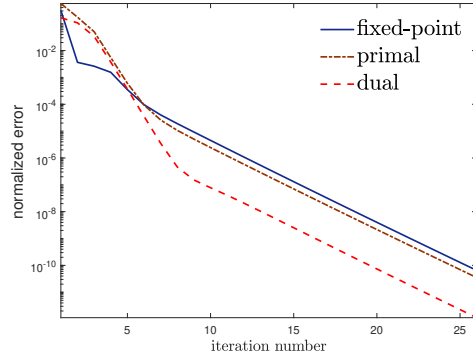


(b) Fixed-point convergence comparison.

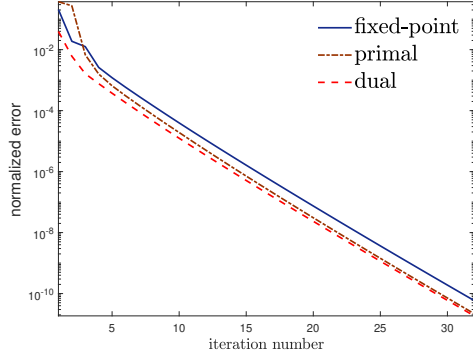
Figure 13: Practical use test (zero initialization).



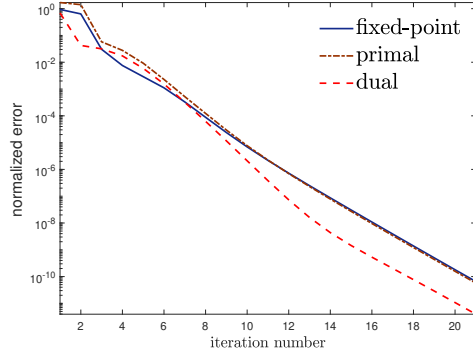
(a) warm-start: $\epsilon_{\text{err}1}, \epsilon_{\text{err}2} \sim \mathcal{N}(0, 0.1)$.



(b) primal warm-start: $\epsilon_{\text{err}1} \sim \mathcal{N}(0, 0.1)$.



(c) dual warm-start: $\epsilon_{\text{err}2} \sim \mathcal{N}(0, 0.1)$.



(d) random initialization $\mathcal{N}(0, 1)$.

Figure 14: Practical use test (non-zero initialization, $\rho_0 = 1$).

Remarks A.4. Under this specific setting for QP, we note that different settings perform similarly, implying a well-conditioned nature.

A.3 Total variation

Consider the following total variation problem:

$$\text{minimize } \frac{1}{2} \|\mathbf{x} - \mathbf{b}\|^2 + \alpha \sum_i |x_{i+1} - x_i| \quad (\text{A.4})$$

with variable $\mathbf{x}, \mathbf{b} \in \mathbb{R}^{100}$. \mathbf{x} is first set to be a ones vector and then randomly scaled on randomly selected entries. \mathbf{b} is set to equal to $\mathbf{x} + \epsilon$, where ϵ is an additive Gaussian noise from $\mathcal{N}(0, 1)$. Regularization parameter is set $\alpha = 5$. Moreover, term $\sum_i |x_{i+1} - x_i|$ can be compactly written into $\mathbf{D}\mathbf{x}$, where we use the popular notation \mathbf{D} to denote a difference matrix, corresponding to our operator \mathcal{A} .

A.3.1 zero initialization

Set initialization $\mathbf{x}^0 = \mathbf{0}, \lambda^0 = \mathbf{0}$.

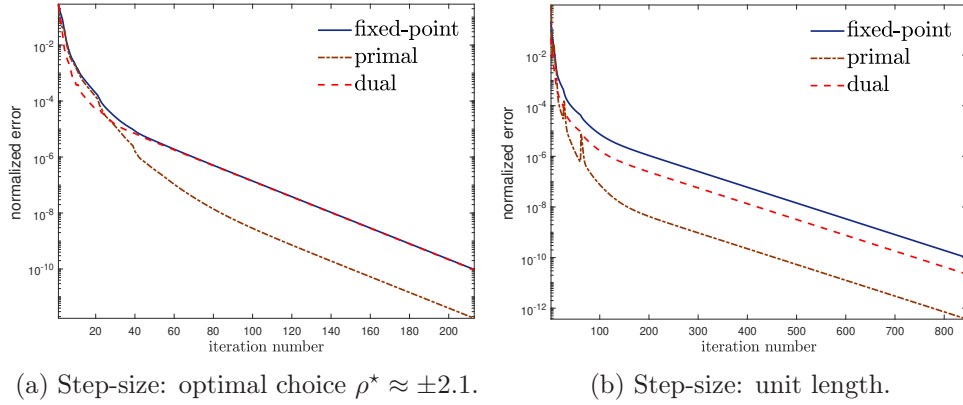


Figure 15: Theoretical results test (zero initialization).

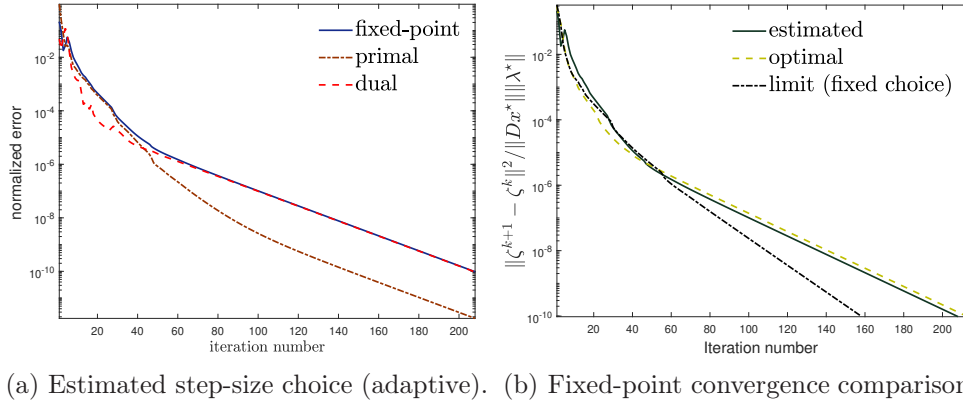


Figure 16: Practical use test (zero initialization).

Remarks A.5. While the optimal choice is quite close to the unit length, it makes a big difference for this application, yielding a $4\times$ acceleration. This is a big improvement due to the data is relatively well-conditioned. Indeed, from Fig. 16b, we see that the limit (for fixed step-size) is with iteration 158, and we achieved 213 without any tailored structure exploited.

A.3.2 non-zero initialization

Set non-zero $\zeta^0 \neq \mathbf{0}$ according to the 4 strategies at the beginning of the appendix.

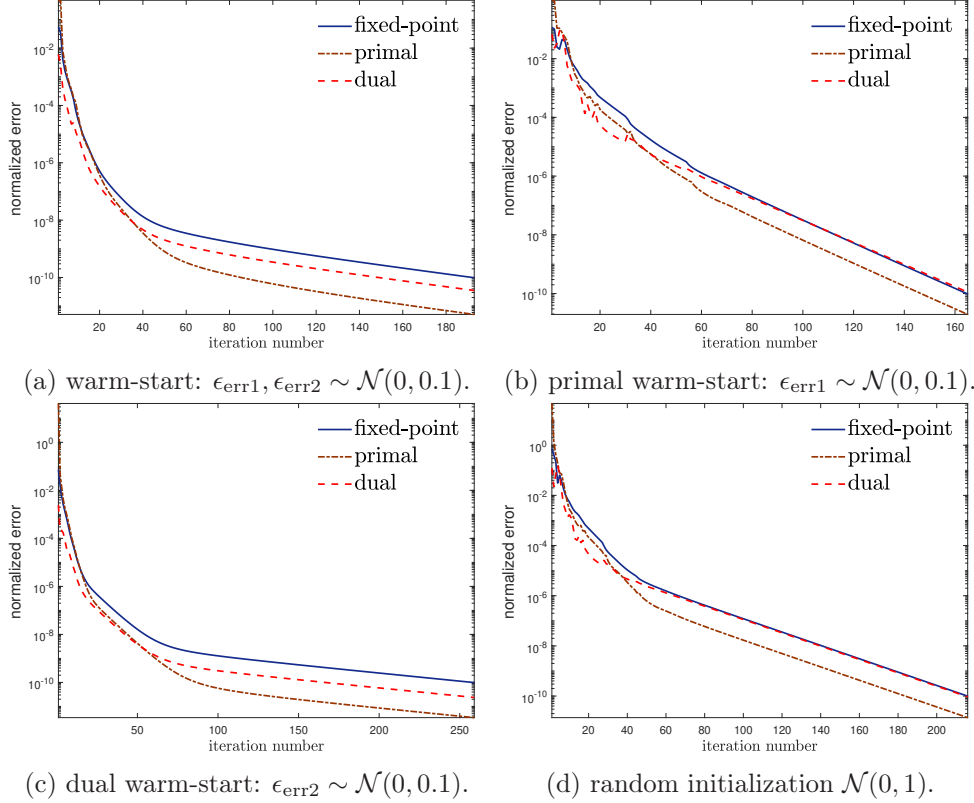


Figure 17: Practical use test (non-zero initialization, $\rho_0 = 1$).

Remarks A.6. Compared the above to the previous zero initialization case in Fig. 16a, we see that the $\mathcal{N}(0, 0.1)$ -type warm start does slightly improve the performance. Moreover, under the current setting, we observe that the primal warm-start strategy performs the best.